SANDIA REPORT
SAND2014-1170
Unlimited Release
Printed February 2014

Fukushima Daiichi Unit 1 Uncertainty Analysis -- Preliminary Selection of Uncertain Parameters and Analysis Methodology

Jeff Cardoni and Donald Kalinich

Prepared by
Sandia National Laboratories
Albuquerque, New Mexico 87185 and Livermore, California 94550

Sandia National Laboratories is a multi-program laboratory managed and operated by Sandia Corporation, a wholly owned subsidiary of Lockheed Martin Corporation, for the U.S. Department of Energy's National Nuclear Security Administration under contract DE-AC04-94AL85000.

Sandia National Laboratories

Issued by Sandia National Laboratories, operated for the United States Department of Energy by Sandia Corporation.

Printed in the United States of America. This report has been reproduced directly from the best available copy.

Available to DOE and DOE contractors from
U.S. Department of Energy
Office of Scientific and Technical Information
P.O. Box 62
Oak Ridge, TN 37831

Telephone:	(865) 576-8401
Facsimile:	(865) 576-5728
E-Mail:	reports@adonis.osti.gov
Online ordering:	http://www.osti.gov/bridge

Available to the public from
U.S. Department of Commerce
National Technical Information Service
5285 Port Royal Rd.
Springfield, VA 22161

Telephone:	(800) 553-6847
Facsimile:	(703) 605-6900
E-Mail:	orders@ntis.fedworld.gov
Online order:	http://www.ntis.gov/help/ordermethods.asp?loc=7-4-0#online

SAND2014-1170
Unlimited Release
Printed February 2014

Fukushima Daiichi Unit 1 Uncertainty Analysis -- Preliminary Selection of Uncertain Parameters and Analysis Methodology

Jeff Cardoni and Donald Kalinich
Sandia National Laboratories
P.O. Box 5800
Albuquerque, New Mexico 87185-MS0748

Abstract

Sandia National Laboratories (SNL) plans to conduct uncertainty analyses (UA) on the Fukushima Daiichi unit (1F1) plant with the MELCOR code. The model to be used was developed for a previous accident reconstruction investigation jointly sponsored by the US Department of Energy (DOE) and Nuclear Regulatory Commission (NRC). However, that study only examined a handful of various model inputs and boundary conditions, and the predictions yielded only fair agreement with plant data and current release estimates. The goal of this uncertainty study is to perform a focused evaluation of uncertainty in core melt progression behavior and its effect on key figures-of-merit (e.g., hydrogen production, vessel lower head failure, etc.). In preparation for the SNL Fukushima UA work, a scoping study has been completed to identify important core melt progression parameters for the uncertainty analysis. The study also lays out a preliminary UA methodology.

ACKNOWLEDGEMENTS

The authors would like to acknowledge the U.S. Department of Energy's Office of Nuclear Energy for providing the funding which supported this work.

CONTENTS

FIGURES

TABLES

ACRONYMS

1F1	Fukushima Daiichi unit 1
1F2	Fukushima Daiichi unit 2
1F3	Fukushima Daiichi unit 3
ANS	American Nuclear Society
BAF	bottom of active fuel
BUR	MELCOR burn package
BWR	boiling water reactor
CAV	MELCOR cavity package
COR	MELCOR core package
CVH	MELCOR control volume hydrodynamics package
DCH	decay heat / MELCOR decay heat package
DDET	discrete dynamic event tree
DHRS	decay heat removal system
DOE	Department of Energy
DW	drywell
ECCS	emergency core cooling system
EOP	emergency operating procedures
EPRI	Electric Power Research Institute
FL	MELCOR flow path package
FW	feedwater
HS	MELCOR heat structure package
IC	isolation condenser
I&C	instrumentation and control
LOCA	loss of coolant accident
LWR	light water reactor
MCCI	molten corium-concrete interactions
MELCOR	NRC severe accident code (not an acronym)
MSIV	main steam isolation valve
NRC	Nuclear Regulatory Commission
PRA	probabilistic risk assessment
PWR	pressurized water reactor
RCS	reactor coolant system
RHR	residual heat removal system
RN	MELCOR radionuclide package
RPV	reactor pressure vessel
SAMG	severe accident management guideline
SOARCA	State of the Art Reactor Consequence Analysis
SBO	station blackout
S/C	suppression chamber (i.e., wetwell)
SNL	Sandia National Laboratories
SRV	safety relief valve
SGTS	standby gas treatment system
TAF	top of Active Fuel
TEPCO	Tokyo Electric Power Company

UA	Uncertainty analysis
WW	Wetwell (i.e., suppression chamber)

1 OVERVIEW

Sandia National Laboratories (SNL) plans to conduct uncertainty analyses (UA) with a MELCOR [1] model of the 1F1 reactor. This model was previously developed for an accident reconstruction investigation jointly sponsored by the US Department of Energy (DOE) and Nuclear Regulatory Commission (NRC) [2]. However, this study only examined a handful of various model inputs and boundary conditions, and the predictions yielded only fair agreement with plant data and release estimates. Further MELCOR Fukushima modeling efforts [3][4][5] proceeded at SNL in a similar fashion–that is, only analyzing a few simulations–and these simulations resulted in better agreement with plant data and release estimates.

The severe accidents at Fukushima Daiichi units involve high levels of uncertainty in accident progression and consequence, as evident by the numerous international accident analyses that all predict various degrees of plant damage and radioactivity releases [2][6][7][8][9][10][11]. Because each analysis employs different plant nodalizations, physics models (if different codes are used), and boundary conditions, every analysis predicts unique accident progressions with varying degrees of agreement with data. Inevitably, the inherent uncertainty and complexity of severe accidents forces analysts to adjust model inputs and boundary conditions in order to "match" data. The SNL Fukushima UA project intends to improve upon these previous forensic analysis methods by taking a more disciplined and methodical approach to severe accident uncertainty.

A thorough forensic understanding of these complicated accidents entails rigorous uncertainty analyses. More than two years after the accidents, many events and operator actions remain unknown. Moreover, key severe accident phenomena are not fully understood and some computational models therefore involve high degrees of uncertainty. Since these accidents are of critical importance to the future of nuclear safety and the use of nuclear power, uncertainty analyses are required to gain a better understanding of the Fukushima accidents. These analyses also provide an opportunity for validation of severe accident codes, which build confidence in the codes and in the guidance derived from their results with respect to reactor decommissioning and severe accident management.

A scoping study has been completed to identify important parameters to be used in uncertainty analyses of existing MELCOR models for the 1F1 reactor. The identification of important uncertain parameters is informed by a previous MELCOR uncertainty analyses for a long term station blackout (SBO) scenario for a MELCOR model of the Peach Bottom; this model was developed for the NRC's State of the Art Reactor Consequence Analysis (SOARCA) project [13]. There exist some similarity between the SOARCA SBO scenarios and the actual accident scenarios that occurred at Fukushima Daiichi. The accident at 1F1 involved limited use of the isolation condenser (IC) system; its accident progression signature resembles the short term SBO scenarios from the SOARCA studies on Peach Bottom, albeit with significant differences due to different reactor designs, safety systems, and mitigation actions by the operators.

In light of substantial differences between the Peach Bottom and Fukushima plant designs and accident scenarios, which are discussed in this introduction, an "outside-the-box" view is taken in identifying key uncertain parameters that were not considered in the SOARCA studies. Particular importance is placed on MELCOR inputs that drive core melt progression and have order-of-magnitude impacts on severe accident phenomena – these include inputs for the modeling of core degradation, in-vessel oxidation, radionuclide release from fuel, radionuclide transport throughout the plant, fission product retention in the reactor pressure vessel (RPV) and containment, and fission product scrubbing in the suppression chamber (S/C) (i.e., wetwell (WW)). Uncertainty in the modeling the failure of certain components, such as safety relief valves (SRV) and main steam lines (MSLs), is central in this effort. Furthermore, considerable uncertainty exists in the treatment of modeling failure in the RPV/RCS (i.e., lower head) due to thermal-mechanical loading of core debris, and failure of the containment due to over-pressurization. However, initial uncertainty studies for 1F1 will likely focus on parameters that have first-order effects on in-vessel accident progression, including boundary conditions such as the (ad-hoc) emergency coolant injection by the operators.

1.1 Purpose of this Report

The purpose of this report is to document the preliminary selection of uncertain parameters and uncertainty analysis methodology that will be used to perform an uncertainty analysis on the 1F1 reactor. When completed, this report will be provided to stakeholders (e.g., DOE, NRC, EPRI, BSAF participants, etc.) for their review and comments. It is expected that, based on the comments that will be received as well as further insights that will be developed as the analysis is performed, the final set of set of uncertain parameters and the uncertainty analysis methodology will be somewhat different from what is documented herein. Hence, while this document has been finalized so as to make it available external to SNL, it should be considered to be a "draft", and that an updated version which incorporates stakeholder comments will be issued as part of the final documentation of the 1F1 uncertainty analysis.

1.2 Peach Bottom SOARCA Uncertainty Study and Comparison to Fukushima Daiichi

Many techniques have been developed to perform uncertainty analyses–several are presented in Helton et al. [14]. The method specifically used in the SOARCA UA is discussed in detail in Appendix A of the Peach Bottom UA documentation [15]. A similar theoretical approach will likely be utilized for the Fukushima UA work.

The SOARCA MELCOR model of Peach Bottom is a 3514 MWt BWR/4 reactor with a Mark-I containment design. The hydrodynamic and structural modeling of the entire plant (core, RPV, RCS, containment, etc.), along with the decay heat and radionuclide inventory modeling of the irradiated fuel, is accomplished using detailed proprietary plant design and performance information. The SOARCA Peach Bottom model is therefore considered a rather detailed and accurate MELCOR representation of a nuclear power plant for severe accident simulations. Nonetheless, given the inherent uncertainty in the nature of severe accidents, MELCOR simulations still involve a considerable degree of uncertainty in their predictions of core degradation/oxidation, RPV damage, containment damage, and radionuclide release/transport.

This uncertainty stems from wide variations in uncertain boundary conditions and high uncertainty in certain phenomenological models in the code.

Boundary conditions for severe accident simulations are by definition difficult to determine–they include extreme initiating events, unanticipated equipment behavior (including failures), and unpredictable operator actions. The severe accidents at Fukushima Daiichi exemplify these features [2]; some examples that were never predicted in traditional probabilistic risk assessments (PRA) and severe accident models are:

- Temporary use of the isolation condensers (ICs) at 1F1, followed by manual termination and subsequent inability to restart the system once DC power was lost due to the tsunami. It is believed that the operators were concerned with cooling down the RPV too rapidly (due to vessel stress reasons–the operators were likely unaware of the coming tsunami) or perhaps because IC operation created a potential containment bypass flow path directly to the environment [2][3][6][8].
- Nearly 70 hours of continuous RCIC operation at 1F2 while operating outside of the RCIC system design space [2][4][6][8],
- At least 30 hours of combined RCIC and HPCI operation at 1F3, including several hours of HPCI operation at very low RPV pressure [5][6][8][10][11],
- 20 hours of continuous cycling of a single SRV at 1F3, potentially causing asymmetric thermal behavior in the S/C including axial stratification or localized saturation [2][5][6][8][9][10][11],
- Mitigative operator actions at each unit that resulted in partial success. This includes containment venting, ad-hoc core injection that did not preclude core damage but may have inhibited further damage such as containment liner melt-through, and containment sprays [2][5].

In comparison to the Peach Bottom SOARCA accident sequences, those at Fukushima exhibited wide variations in event timing (e.g. emergency core injection after/during core damage) and magnitudes (e.g. significant leakage of injection water due to ad-hoc piping networks) [2].

Phenomenological uncertainty resides primarily in the MELCOR physics models for core damage and in-vessel material relocation. These models are informed by a limited number of experiments such as Phebus [16], the SNL DF-4 program [22], and the SNL XR2-1 experiments [23]. The melt progression of a large reactor core is not a fully understood phenomenon; it is complicated by tightly coupled, time-dependent thermal-hydraulics, chemistry (e.g. oxidation), material interactions, and perhaps neutronics–all under conditions of rapidly evolving geometry, temperature, and pressure. Therefore, the computational models in MELCOR (as in most other severe accident codes) for gross core damage are semi-mechanistic, two-dimensional, lumped parameter treatments [1]. Despite this simplified approach, the in-vessel damage progression is usually the most computationally challenging portion of a MELCOR simulation.

1.3 Accident Sequence and Operator Mitigative Actions

The large uncertainties involved with accident sequence variables and operator actions are discussed in Section 4. These parameters are outside the realm of MELCOR's predictive capabilities, but are still required to be "modeled" to some degree in the severe accident simulation. Therefore, uncertain parameters pertaining to accident sequence effects and operator actions will be treated mostly as boundary conditions in the UA. That is, the influence these parameters have on accident progression, source term, and consequence should be quantified separately from other uncertain parameters. Otherwise these boundary conditions tend to engulf the quantitative effects of other uncertain parameters.

To some degree, the SOARCA-UA for Peach Bottom exhibited uncertain parameter "washout" by including accident sequence parameters simultaneously with physics model parameters. This does not suggest that uncertainty in accident sequence should not be quantified, or that the SOARCA-UA was in error in its approach. Instead, for uncertainty analysis for a real severe accident such as 1F1, which in reality proceeded down a single specific accident sequence path, it is beneficial to separate the quantitative effects of physics model uncertainties from accident sequence uncertainties. This approach will facilitate the comparison and perhaps validation of the physics models in MELCOR against plant data, especially as the reactors are decommissioned and more data is made available (e.g., the conditions of the cores). Also, this will allow for easier assessments of MELCOR model predictions against other severe accident codes such as MAAP.

The distinction between boundary condition and model input/prediction is not always a clear one. For example, MELCOR has the capability to predict the generation of hot steam and gases (e.g., H_2) in the core, which in turn flow through the steam lines as SRVs cycle due to high pressures. In conjunction with high system pressure, these gases can challenge the integrity of certain RCS components such as the SRVs or the MSLs. MELCOR does not perform a detailed 3D failure simulation of these components like a finite element analysis code would do. However, it can perform Larson-Miller calculations for creep rupture. The creep rupture model incorporates volumes and a 1-D heat structure representing the component, thereby obtaining the local time-dependent temperature and pressure from the MELCOR CVH/FL/HS packages. It also uses material-specific properties and 1-D stress calculations for the calculation of the Larson-Miller parameter. Although this treatment requires very little computational expense (i.e., it is simple) compared to the bona fide physics models in MELCOR, it is an engineering approach to modeling component failures that are important to severe accidents. Thus the question of "did MELCOR predict an RCS failure?" is ambiguous and arguably a philosophical classification–MELCOR performed mechanistic calculations for mass, energy, momentum, and the generation of hot gases, and then used a relatively simple model as an "dynamic boundary condition" to simulation failure of an RCS component.

1.4 Scope of Fukushima UA

Given the project's scope and schedule, only the 1F1 reactor will be evaluated in this Fukushima UA. It was chosen for the UA as its accident progression better understood than those for 1F2 and 1F3. Also, from a tractability standpoint, the 1F1 MELCOR model runs much faster than those for 1F2 and 1F3, and it is much more robust in terms of code convergence errors.

Although not analyzed in this analysis, this report does contain some 1F2 and 1F3 information. It has been included in the report for comparative purposes and as a place-holder if this work is ever extended to those models.

1.5 Report Structure Summary

Section 2 of this report provides a brief summary of relevant design features of the Fukushima plants and the development of the MELCOR models. A short review of the Peach Bottom SOARCA uncertainty analysis is given in Section 3. Boundary condition uncertainty (i.e., uncertainty in the accident sequence) is discussed in Section 4, while uncertainty in the core phenomenological model input is discussed in Section 5. Computation uncertainty is discussed in Section 6. The preliminary uncertainty analysis methodology is described in Section 7; this includes a summary of the uncertainty parameters and the analyses that will be performed. A summary of the report is provided in Section 8.

2 PLANT DESIGN AND MODEL DEVELOPMENT REVIEW

Unit-specific plant models are required to perform MELCOR uncertainty studies for comparison to real events and plant data. A general overview of the 1F1 reactor, RPV, RCS, containment, and safety systems is provided here. Brief summaries of the components of the MELCOR model development from previous work [2] are also discussed. Although the initial Fukushima UA studies will likely focus on 1F1, plant data for 1F2 and 1F3 are included.

2.1 RPV and RCS

1F1 is an older BWR/3 design. It has significantly smaller core, RPV, RCS, and containment dimensions (compared to the 1F2, 1F3, or Peach Bottom plants), which are important for severe accident models. It is for these reasons that unique RPV, RCS, and containment models were created for each unit in the joint DOE/NRC project [2]. These unit-specific models were created using the best available plant data at the time. Additional RCS and RPV dimensions have become available since this work was completed, including steady state plant performance data (e.g. recirculation flow rate) that were previously unknown and estimated (i.e., downscaled) from Peach Bottom data. The MELCOR models for the uncertainty analyses will be updated with the latest plant geometry data, and steady state code predictions will be benchmarked against data. SNL previously developed the ability of automated generation of RPV input for each Fukushima unit [2], which will facilitate any uncertainty analyses of the RPV models (e.g., nodalization uncertainties).

Even though 1F1 is an older BWR/3 design, it still uses the same basic RCS configuration of 4 steam lines, 20 jet pumps, 2 recirculation loops/pumps, and 2 feedwater lines, as shown in Table 1.

Table 1. Reactor Core Design Data for Fukushima and Peach Bottom Reactors.

Parameter	1F1	1F2 and 1F3	Peach Bottom SOARCA
Vessel diameter (m)	4.78	5.60	6.38
Vessel height (m)	18.86	21.7	22.2
Vessel thickness (m)*	0.165	0.145	0.1635
# of recirculation loops/pumps	2	2	2
# of jet pumps	20	20	20
# of steam lines	4	4	4
# of feedwater lines	2	2	2
Core flow rate (t/hr)	21800	33800	46750
Bypass flow (t/hr)	2180	3380	7300
Steam flow (t/hr)	2140	4440	6520
Avg. core temperature (K)	558	559	561
Lower head CRD tube diameter (m)	0.15	0.15	0.27
Lower head SRM/IRM tube diameter (m)	0.051	0.051	0.0503
Core SRM/IRM tube diameter (m)	0.015	0.015	0.0178
RPV operating pressure (MPa)	6.99	7.03	7.23
Recirculation flow rate (t/hr)	5600	7570 / 7760	7860
Recirculation pump head (m)	103.6	153 / 152.4	216
Recirculation pipe diameter (m)	0.61	0.712	0.6795
Main steam pipe diameter (m)	0.40	0.61	0.61

* RPVs are composed of different steels between 1F1 and 1F2/1F3. The bulk RPV steel for 1F1 is ASME SA 302B, ASME SA 336. The bulk RPV steels for 1F2 and 1F3 are ASME A 533Gr.B.C1.1, ASTMA 508 C1.2. All units have a 5 mm stainless steel clad on the interior of the RPV wall (stainless steel grade was not specified by TEPCO).

2.2 Containment

All Fukushima units of interest share the same Mark-I containment design as the Peach Bottom plant analyzed in the SOARCA-UA. Relatively minor geometry differences in the form of overall drywell and wetwell fluid volumes have been reflected in the unit-specific Fukushima models developed in the DOE/NRC project [2]. Minor uncertainties may exist important for severe accident simulations, such as the initial wetwell pool water level and temperature at the time of scram. SNL previously developed the capability to automatically generate containment input for each Fukushima unit [2], which will facilitate any uncertainty analyses of the containment models such as nodalization uncertainties. However, detailed geometric information of the containment cavities is still not available, and thus geometric dependence of ex-vessel MCCI and debris movement remain highly uncertain.

Concerning containment failures, 1F1 seems to exhibit a containment pressure trend resembling head flange leakage; that is, containment pressure increases and levels out around 0.75-0.80 MPa for about 8 hours, after which the wetwell is vented and the containment depressurizes (followed by the reactor building explosion) [2][3]. The Peach Bottom SOARCA UA model assumed the containment head flange begins leaking around 0.65 MPa, based on a rather rudimentary mechanical analysis of the DW head flange bolts [15]. Consequently, the MELCOR 1F1 model assumed a different pressure vs. leak area curve in order to match TEPCO pressure data. Containment leakage remains a highly uncertain boundary condition for the MELCOR Fukushima models.

2.3 Safety Systems

Being an older BWR/3 reactor, 1F1 has a significantly different collection of safety systems compared to 1F2, 1F3, and Peach Bottom. 1F1 has ICs instead of RCIC, and lacks the residual heat removal system (RHR) that includes lower pressure core injection (LPCI, separate from core sprays), and containment sprays. Instead, 1F1 has different shutdown cooling (SHC/SDC) and containment spray systems, as shown in Table 2.

1F2 and 1F3 have the same safety systems as Peach Bottom. However, there still exist differences such as flow rates, water capacity, piping sizes, heat transfer capacity, and pump head. Furthermore, there exist considerable uncertainties in how these systems actually performed and how they were manipulated by the operators. The RCIC at 1F2 and the HPCI at 1F3 are known to have operated for many hours in off-nominal conditions such as excessively high RPV water level (1F2) and very lower RPV pressure (1F3).

Table 2. Safety System Information.

System	1F1 (BWR/3)	1F2/1F3 (BWR/4)	Peach Bottom (BWR/4)
RCIC		✓	✓
RHR		✓	✓
LPCI		✓	✓
IC	✓		
SHC/SDC*	✓		
HPCI	✓	✓	✓
Core Sprays	✓	✓	✓
DW/WW Sprays	✓	✓	✓

*Shutdown cooling system is unique to 1F1 and is similar in purpose to the RHR system of 1F2, 1F3, and Peach Bottom. This system is not modeled in the 1F1 MELCOR model since it does not appear to have been activated during the accident.

3 PEACH BOTTOM SOARCA UNCERTAINTY ANALYSIS

Since the Peach Bottom and Fukushima reactors are relatively similar, the Peach Bottom SOARCA-UA provides a good foundation for uncertainty analyses of the MELCOR Fukushima models. Besides providing a starting basis for the identification of BWR severe accident uncertainty parameters, the framework and software tools developed for the SOARCA UA carry over well to the Fukushima UA.

Figure 1 shows the procedural framework developed for the SOARCA UA. A base MELCOR input deck and the chosen uncertain parameters are passed into the MELCOR uncertainty engine. In a highly automated fashion, the uncertain parameters (some SOARCA-UA examples are shown in the red boxes) are sampled using simple random sampling with the appropriate probability distributions, and the sampled values are implemented into N number (the number of samples/realization) of generated MELCOR input decks. The final results for the SOARCA-UA examined 3 replicate cases[1] with 300 samples each using simple random sampling.

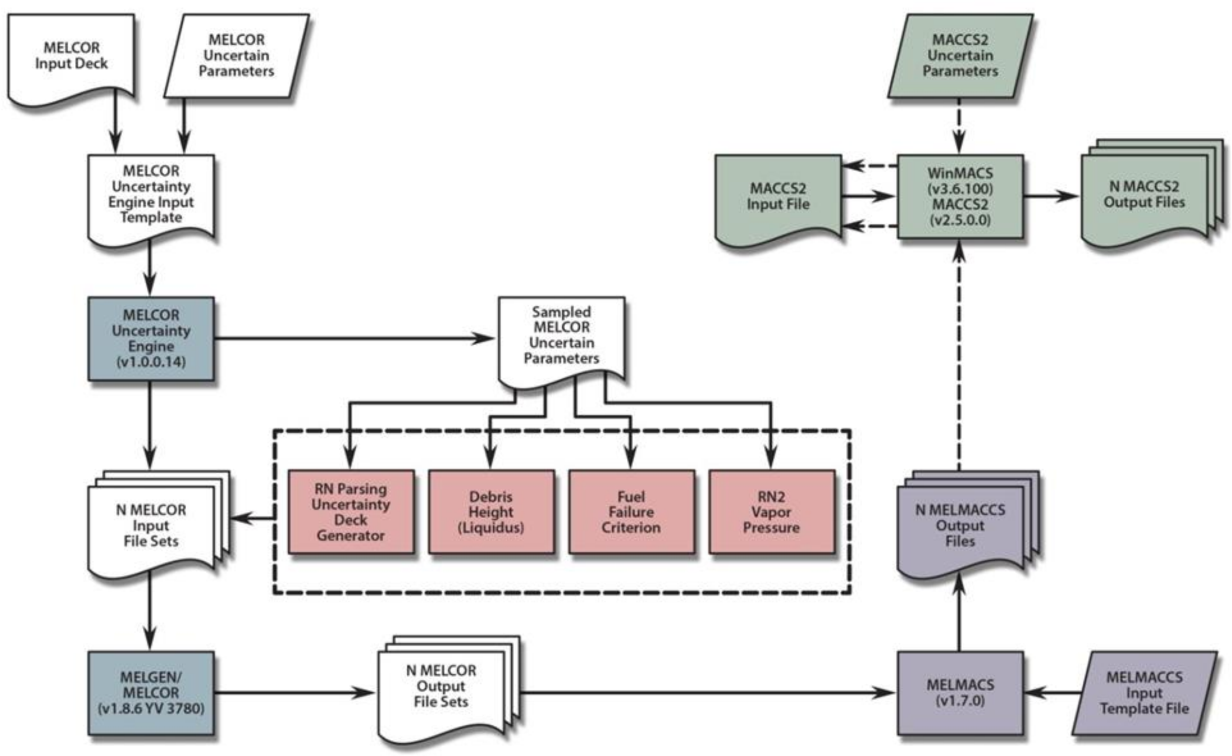

Figure 1. Peach Bottom SOARCA UA MELCOR/MACCS Flow Diagram.

[1] A replicate case is one in which the uncertainty analysis is rerun with a different seed for the random number generator. Using a different seed results in a different set of sampled uncertain parameter values.

The Peach Bottom SOARCA-UA project examined 21 MELCOR parameters and 350 MACCS parameters (representing 20 parameter groups) in the integrated analysis. Some of these parameters are listed in Table 3. For the Fukushima UA work, certain in-vessel accident progression parameters will likely be adopted from the SOARCA-UA, namely the Zircaloy melt breakout temperature, the molten clad drainage rate, and the radial debris relocation time constants. Different approaches will likely be taken concerning SRV seizure, MSL rupture, and ex-vessel behavior, given the known accident signatures from the Fukushima plants. For example, containment pressure data suggests that none of the containments were permanently compromised, which would be evident by a permanent depressurization to atmospheric pressure. Hence, ex-vessel modeling and uncertain parameters will likely be modified to reflect this data.

Table 3. Peach Bottom SOARCA UA MELCOR and MACCS Uncertain Parameters.

MELCOR	MACCS2
Epistemic Uncertainty	**Epistemic Uncertainty**
Sequence Issues	***Deposition***
SRV stochastic failure to reclose	Wet deposition model
Battery Duration	Dry deposition velocities
In-Vessel Accident Progression Parameters	***Shielding Factors***
Zircaloy melt breakout temperature	Shielding factors
Molten clad drainage rate	***Early Health Effects***
SRV thermal seizure criterion	Early health effects
SRV open area fraction	***Latent health effects***
Main Steam line creep rupture area fraction	Groundshine
Fuel failure criterion	Dose and dose rate effectiveness factor
Radial debris relocation time constants	Mortality risk coefficient
Ex-Vessel Accident Progression Parameters	Inhalation dose coefficients (radionuclide specific)
Debris lateral relocation – cavity spillover and spreading rate	***Dispersion Parameters***
Containment Behavior Parameters	Crosswind dispersion coefficients
Drywell liner failure flow area	Vertical dispersion coefficients
Hydrogen ignition criteria	***Relocation Parameters***
Railroad door open fraction	Hotspot relocation
Drywell head flange leakage	Normal relocation
Chemical Forms of Iodine and Cesium	***Evacuation Parameters***
Iodine and Cesium speciation fractions	Evacuation delay
Aerosol Deposition	Evacuation speed
Particle Density	**Aleatory Uncertainty**
	Weather Trials (x984)

4 BOUNDARY CONDITION UNCERTAINTIES

By definition, severe accidents for nuclear reactors involve large uncertainties in the boundary conditions imposed on the plant during the accident. The external events and assumed operator actions for hypothetical severe accident scenarios, such as those in SOARCA, are unanticipated with regards to design basis accidents and are therefore uncertain. For real-life severe accidents such as Fukushima, some external events become well-quantified such as the time of scram due the seismic event and the timing of the tsunamis, which knocked out most electrical power. However, later external events and the effects of operator actions remain extremely uncertain due to a lack of reliable instrumentation and the stress of the situation. Operators can hardly be expected to keep quality logbooks of circumstances during severe events with no power (i.e. no lights or instruments) and little outside support given the utter chaos caused by the tsunamis wiping out large sections of infrastructure in the surrounding area. Years after such catastrophes, the precise behavior of key systems (e.g. RCIC and HPCI) and the associated operator actions (e.g. throttling and containment venting) remain indeterminate, especially for accident scenario reconstruction scenarios. Therefore severe accident and consequence simulations with MELCOR and MACCS naturally develop into uncertainty analyses.

This section describes potential uncertain parameters that are best described as boundary conditions for the MELCOR code; detailed and mechanistic models internal to MELCOR are not available to describe these systems in any formal/scientific manner. However, this does not necessarily mean that the modeling of these parameters in MELCOR must be completely static. Simple MELCOR models, or user-defined model via MELCOR control functions, may provide some level of predictive capability for these parameters. Nonetheless, the parameters described here involve such inherent uncertainty to require being modeled as dynamic boundary conditions in MELCOR.

4.1 Initiating and External Events – Associated Immediate System Response

There are a number of immediate system response parameters that are uncertain in the Fukushima accident sequences. These include:

- MSIV closure time
- feed water pump coast down flow rate
- recirculation pump coast down flow rate
- recirculation pump leakage

At this time these parameters will be characterized by point estimates. They are included as a place holder in the event that after the review of this document it is decided to include them in the uncertainty analysis. SNL MELCOR simulations to date have determined that these parameters have relatively weak influence on in-vessel accident progression, since core uncovery starts hours after shutdown (about 3 hours for 1F1, 75 hours for 1F2, and 35 hours for 1F3).

However the behaviors of these systems do have a strong effect on early RPV and containment pressure response.

4.2 Unknown System Behaviors and Failures

4.2.1 Functioning of ICs

The initial operation of the ICs is well-characterized by the 1F1 operation logs. However, there is some uncertainty regarding whether the ICs actually functions after the tsunami (despite the operators taking action to actuate them) and if they did operate, how was their performance potentially impacted by non-condensable gases (e.g., hydrogen) produced due to uncovering and heat up of the cladding.

At this time IC operation will be treated in the same manner as in the original SNL 1F1 analysis [2, Table 1], where IC operation after the tsunami is ignored under the assumption that the system was not actually activated or that the presence of non-condensable gases caused significant degradation of their performance such that it had little to no impact on the accident progression.

4.2.2 Modes of RPV Depressurization and RCS Pressure Boundary Failure

There are a number of modes of RPV depressurization failure that have been postulated as in previous SNL BWR severe accident analyses and from Fukushima analyses performed by TEPCO.

- main steam line failure
- safety relief valve failure
- safety relief valve grapfoil seal failure

Main steam line failure has been modeled with a Larson-Miller treatment of creep rupture [13]. This treatment accounts for stress and temperature via a fraction lifetime rule. It also will capture failure from reduction in yield strength due to very high temperatures. The rupture area of the failed main steam line has been characterized as most likely being on the same order as the main steam line pipe diameter, with a smaller probability of being

SRV failure has been evaluated as occurring from excessive cycling or from heat-up of the valve. [13]. Failure due to valve cycling has been treated as a stochastic process which is quantified (in terms of number of cycles until failure) based on limited valve failure data. Failure due to valve high temperature assumes that at or above an elevated threshold temperature (based on the valve material properties) portions of the valve may begin to deform. In both cases the valve is assumed to fail open. The analyses performed by TEPCO have postulated failure of an SRV grapfoil gasket due to high temperature as a potential mechanism for RPV depressurization. Failure of the gasket is assumed to occur at its maximum design temperature of 723 K. Failure of the gasket is assumed to result in a leak area of 0.000858 m^2.

While all of the above RPV depressurization mechanisms could be evaluated in terms of physics-based uncertainty (e.g., uncertainty in temperature threshold, Larson-Miller parameter uncertainty, material property uncertainty), an alternative is to simply develop an uncertainty distribution for the time of RCS pressure boundary failure and the leakage area associated with it. This characterization includes the effects of small-leak area failures (e.g., grapfoil gasket, SRV) and large-leak area failures (e.g., MSL). It also accounts for temporal variation due to the system's thermal response, as well as uncertainties in material properties, actual failure thresholds, and deviations of the system from its ideal characterization (i.e, unknown flaws).

Looking at the range of 1F1 analyses finds that RCS pressure boundary failure is predicted to occur between 5.5 hr and 6.5 hr. The SRV and MSL temperatures during this time period are in line with the temperatures required for failure. As the purpose of including the variation in the failure time is to assess its impact on the accident sequence, a uniform distribution is suggested with lower and upper bounds of 5.5 and 6.5 hr, respectively.

4.2.3 Containment Failure and Self-Venting

As noted in Section 2.2, the containment pressure signatures from the Fukushima reactors suggest that there are times at which significant containment leakage occurred.

In 1F1 the containment pressure trend appears to resemble head flange leakage. Shortly after the time of initial emergency core injection (15 hr) the containment pressure increases and levels out around 0.75-0.80 MPa until when it is reported that the wetwell was vented (23 hr), at which time the containment depressurizes [2][3]. This behavior is qualitatively consistent with the treatment of head flange leakage in the Peach Bottom SOARCA model.

The uncertainty in head flange leaking in the Peach Bottom SOARCA UA was treated by implementing a simple head flange bolt stress/strain model that accounts for bolt pre-tensioning and head gasket decompression. Uncertainty in the bolt material modulus of elasticity, friction coefficient between the bolt threads and head flange threads, and degree of head gasket decompression were used to characterize the uncertainty in the head flange leakage area.

While this method could be used for the 1F1 UA, assuming Fukushima-specific information was provided, there is also possible that a simple model using a threshold pressure for non-zero leakage and a constant dA/dp relationship above the non-zero leakage threshold could be used. This model would be calibrated against the 1F1 drywell pressure data at the best estimate water injection flow rate (see Section 4.3.1). Uncertainty in both the non-zero leakage threshold pressure and dA/dp would be characterized as uniform. Lower and upper bounds would be defined as +/-10% of the 1F1 base case.

4.3 Operator Mitigative Actions

4.3.1 Emergency Core Injection

The initial values reported for emergency core injection flow rates have subsequently been reassessed and are now considered to overestimate the amount of water that actually reached the RCS. That said, there is no definitive revision to the injection flow rates. Rather, what has occurred is that the injection flow rates have been adjusted in analyses to of the Fukushima accident sequences to “tune” results to match the sparse plant data (e.g., drywell and wetwell pressure, radiation measurements, times of combustion events).

At this time, Fukushima analyses are currently using injection flow rates on the order of 10% to 20% [2][3][4][5] of the initial reported values. It is recommended for this analysis that the initially reported injection flow rates be scaled by a uniform distribution with a lower bound of 0.05 and an upper bound of 0.25.

4.3.2 Containment Venting

Containment venting operations are reported in all of the Fukushima Daiichi accident sequences [2, Tables 1, 2 and 3]. For this analysis, the timing of the 1F1 wetwell venting (at 23.73 hr) will be treated as a point-estimate value identical to that in [2].

4.4 Core Decay Heat and Radionuclide Inventory

As shown in Table 4, the Fukushima reactors[2] are of sufficiently different core design, power rating, assembly type, and burnup level to warrant unit-specific core models for the MELCOR core (COR) and hydrodynamic (CVH/FL) packages. Fukushima unit-specific structural and hydrodynamic models of the fuel assemblies, channel boxes, control blades, core support structure, coolant channels, bypass regions, and lower plenum were completed in the joint DOE/NRC Fukushima analysis project [2].

[2] The MELCOR COR ring nodalization is shown in Figure 2 and Figure 3.

Table 4. Reactor Core Design Data for Fukushima and Peach Bottom Reactors.

Parameter	Fukushima Unit 1	Fukushima Units 2 and 3	Peach Bottom SOARCA
Reactor type	BWR/3	BWR/4	BWR/4
Rating (MWt)	1380	2381	3514
Fuel mass (tHM)	68	94	133
# fuel assemblies	400	548	764
# control blades	97	137	185
Fuel assemblies – type (quantity)	8x8 (68), 9x9B (332)	Unit 2: 9x9B (548) Unit 3: 9x9A (516), 8x8MOX (32)	GE 10x10 (764)
Fuel height, core diameter (m)	3.66 / 3.7	3.71 / 4.4	3.81 / 4.8
Avg. core burnup at shutdown (GWd/t)*	25.8	Unit 2: 23.2 Unit 3: 21.4	MOC: ~24
Peak fuel assembly burnup at shutdown (GWd/t)	41.3	Unit 2: 42.4 Unit 3: 41.7	MOC: ~46

*For the Fukushima reactors, this is the whole-core average burn-up at the time of scram due to the seismic event (3/11/2011 14:46). It is TEPCO data from the plant process computer. For Peach Bottom, this is the middle-of-cycle (MOC) burn-up that is modeled in SOARCA for the core decay power and initial inventory in MELCOR/MACCS.

Late in the development of the Fukushima MELCOR models, TEPCO-calculated core decay power and radionuclide inventories were made available for each unit. The TEPCO decay powers were incorporated into the SNL MELCOR models for each unit [2], but the TEPCO inventories were not implemented. Rather, a power-scaled inventory was adopted from the Peach Bottom SOARCA model. The TEPCO-supplied inventory was not implemented due to the following reasons:

- The inventory was generated by an ORIGEN2 calculation that was separate from the overall core decay heat and power distribution calculations. ORIGEN2 is a deprecated code, and the use of separate analyses for inventory and decay power data reduces the consistency and scrutability of the MELCOR/MACCS models. ORIGEN-S in SCALE is the current US-NRC code of choice for inventory and decay power calculations. It also has access to the latest ENDF/B-VII.0 cross section data.
- The inventory only reflected the whole core inventory and lacked spatial distribution details. Radial distributions of radionuclides are especially important for cores where older, high burn-up fuel assemblies are shuffled predominately to the periphery of the core, which was the case for 1F1.
- The TEPCO inventory specified nuclide activities for actinides, fission products, and light activation products, which are indeed necessary information for MELCOR and MACCS. However, by nuclide masses, a large portion of the initial core inventory of fission products (and some activation products) and their decay daughters are actually stable–the activity of a stable nuclide is zero and is no longer much concern once a source term calculation is complete. In fact, MACCS only models the consequence effects of certain radioactive nuclides. Still, the stable nuclide masses are very important for the accurate generation of MELCOR radionuclide (RN) inventories and the subsequent transport simulation. Initial inventories for MELCOR RN classes require lumped elemental masses, and the isotopic breakdown of these masses is also required input for MACCS (i.e., MELMACCS input). MELCOR RN classes are lumped physically and chemically, and the code assumes the initial inventories reflect the total class mass in the fuel and in the fuel-clad gap at reactor shutdown. Upon core heat-up and oxidation, fuel temperatures rise and volatile radionuclide classes are rapidly released from the fuel. These radionuclides transport throughout the plant as vapors and aerosols. Overall vapor and aerosol mass are important for accurate radionuclide transport calculations in MELCOR for each RN class. Hence, it is imperative to include stable radionuclide masses that reside in the fuel, such as Cs-133 (~40% of all core cesium) and I-127 (~20% of all core iodine). These stable nuclides are released with the appropriate RN classes and contribute to overall vapor and aerosol masses for the transport calculations.

In light of these discrepancies, SNL has developed an automated method for generating accurate and consistent MELCOR inventories, overall core decay power, MELCOR RN class specific decay powers, and MELMACCS isotopic inventories for each Fukushima unit. ORIGEN-S and Automatic Rapid Processing (ARP for burn-up dependent cross sections, supplied via the TRITON sequence) are used from the SCALE6.1.2 code package [36], along with automation scripts that use fuel assembly-specific data provided by TEPCO. This capability provides a consistent radionuclide inventory for use by MELCOR and MACCS, which is required for integrated MELCOR and MACCS uncertainty analyses.

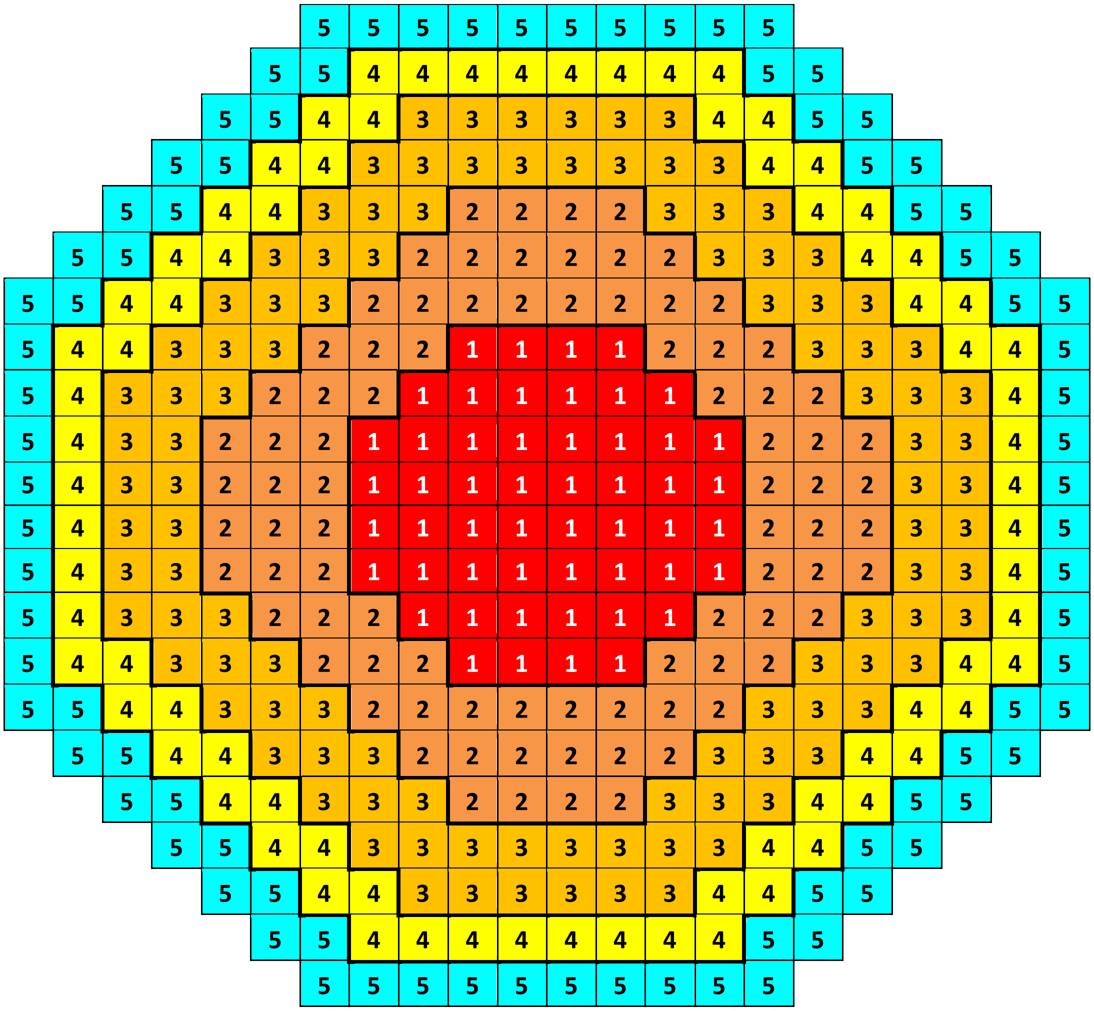

Figure 2. Default 5-ring nodalization scheme of MELCOR COR, CVH, and FL packages for unit 1 core region. The bypass volumes and flow paths are not represented here.

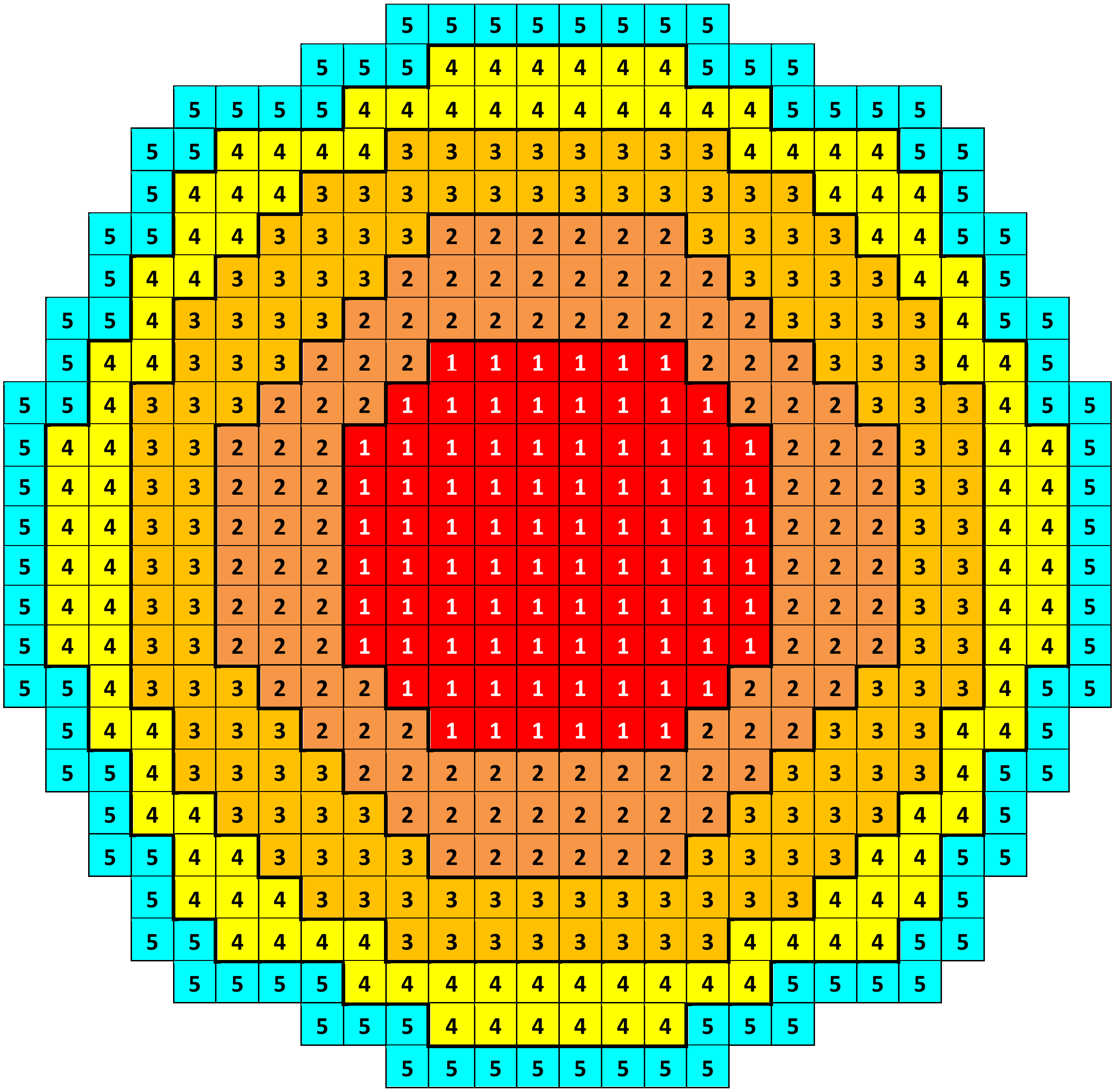

Figure 3. Default 5-ring nodalization scheme of MELCOR COR, CVH, and FL packages for unit 2/3 core region. The bypass volumes and flow paths are not represented here.

The "Decay Heat Power in Light Water Reactor" standard, ANS-5.1-2005, provides a method for calculating a conservative decay heat curve for light water reactors, with associated uncertainties. This standard is primarily used in safety evaluations and is biased toward higher decay heat levels than would be predicted by ORIGEN-S calculations. The Fukushima uncertainty analysis attempts to reconstruct the actual accident conditions to the extent possible, thus applying a conservative decay heat curve would be counterproductive to the overall project goal. While the decay heat curve may be conservative, the uncertainties provided in ANS-5.1-2005 may still be assumed to apply to a best-estimate decay heat uncertainty calculation. A high level description of a hybrid-approach to exploring decay heat uncertainties for the Fukushima reactors is provided here.

Uncertainty in decay heat will be evaluated using a mixture of best-estimate ORIGEN-S generated decay heat curves generated for each reactor and uncertainty within each decay heat curve derived from ANS-5.1-2005. From the ORIGEN-S calculations, fractional fission powers over the previous cycle of important actinides (U-235, U-238, Pu-239, Pu-241) can be extracted. Using these nuclide specific fission power levels the time-dependent uncertainties in percentage of total decay heat power can be calculated using the methods described in Section 3 of ANS-5.1-2005. Once the time-dependent decay heat uncertainties are assessed for the Fukushima units, these uncertainties can be applied to ORIGEN-S generated decay heat curves. Finally, these decay heat curve distributions will be sampled using unbiased Monte Carlo techniques to provide decay heat input records for MELCOR calculations.

5 CORE PHENOMONLOGICAL MODEL INPUT UNCERTAINTIES

Phenomenological uncertainties for severe accident simulations principally deal with core damage, core melt progression and debris relocation (in-vessel and ex-vessel), RPV lower head failure, and any model pertaining to radionuclide behavior. There exists any number of additional uncertain phenomena during severe nuclear accidents, including fundamental treatments of fluid flow and heat transfer. However, in general these models are more mechanistic and better understood than phenomena specific to nuclear fuel damage. Reactor thermal-hydraulics has been extensively studied, even for accident conditions, in the form of decades of experiments and computational analyses; a few of the US codes used for reactor thermal-hydraulics are: RELAP5, RELAP-3D, TRAC, TRACE, and CFD codes such as FLUENT and STAR-CD. Granted, uncertainties remain in these codes, perhaps considerably for certain phenomena (e.g., two-phase turbulent flows), yet these uncertainties are largely dwarfed by those related to severe accident physics. In fact, most thermal-hydraulics uncertainties for severe accidents are plausibly related to the changing geometry due to core/vessel damage. Core damage and material relocation models in severe accident codes have historically been treated in a semi-mechanistic manner, relying heavily on relatively few experiments such as Phebus [16]-[21], the SNL DF-4 program [22], and the SNL XR2-1 experiments [23]. Severe accident experiments with irradiated fuel and at realistic scales are very costly–hence also very rare.

Multi-physics, multi-scale, three-dimensional, and first-principle models of core damage have not been attempted in past severe accident studies, and no such code currently exists to the authors' knowledge. Considering that an ultra-high fidelity direct numerical simulation of fluid flow and heat transfer in a intact core involves over 10^{16} unknowns and requires peta-scale supercomputers [32], all for a single time step solution, these extremely CPU-expensive approaches have not been attempted for severe accident simulations. The continually changing geometry under which fluid flow, heat transfer, material interactions, and chemical reactions take place in severe accidents has necessitated more parametric approaches in codes such as MELCOR. The long time scales of severe accidents are another factor. Severe accident typically last several days to weeks, as exemplified by the Fukushima accidents; in conjunction with governing equations that usually require sub-second time step sizes, a severe accident simulation with MELCOR usually necessitates millions of timesteps [1][5]. Lastly, the intrinsic high uncertainty in the boundary conditions for severe accidents reduces the utility of a costly and ultra-precision computer simulation with a single set of boundary conditions.

5.1 COR Package Sensitivity Coefficients

Severe accidents by definition involve a significant degree of core damage, oxidation, and radionuclide release from fuel. In contrast to design basis accidents, the thermo-mechanical behavior of the core cannot be treated simply as a static 'can' of heat. The behaviors of the fuel and core debris are of primary concern for a severe accident, and dictate the progression of the accident during certain phases. Before RPV lower head failure and debris discharge to the cavity, the in-vessel calculations for fuel and structural debris behavior are simulated by the COR package. Given inherent uncertainties in the modeling of core damage and material relocation, the COR package contains a large number of sensitivity coefficients to facilitate user sensitivity and uncertainty studies. Not every sensitivity coefficient in MELCOR is necessarily indeterminate–some model inputs are implemented as sensitivity coefficients merely to increase code flexibility. For example, data for material properties (e.g. liquidus and eutectic temperatures) are well-quantified in scientific literature but can nevertheless be modified in MELCOR via sensitivity coefficients.

Sensitivity coefficients in MELCOR are categorized by numbers. An overview of the sensitivity coefficients in the COR package is given below:

1001 – 1299:	oxidation, heat transfer, material relocation, component failure, and debris blockage parameters
1301 – 1399:	fission power parameters
1401 – 1499:	numerical control and point kinetics parameters
1501 – 1599:	geometric, convergence, and some blockage parameters
1600 – 1699:	lower-head mechanical model and support structure parameters.

A detailed review of these sensitivity coefficients, along with their associate COR package sub-models, is provided in Appendix A. This review is intended as a reference guide for SNL MELCOR modelers and to expedite the identification of important parameters for the Fukushima UA project. The COR package parameters for the Fukushima UA were selected from the review in Appendix A and are described in further detail in the following sections. Some of these parameters were also considered in the SOARCA-UA work.

5.1.1 Molten Zircaloy Melt Break-through Temperature

As fuel rod temperatures rise during a severe accident, Zircaloy cladding reacts with steam to form outer oxide shells. The oxide shells have a high melting temperature relative to that of unoxidized cladding and, as evidenced in the Phebus experiments, would maintain fuel geometry as Zircaloy interior to the shell melted and drained away [1][15]. This configuration is illustrated in Figure 4.

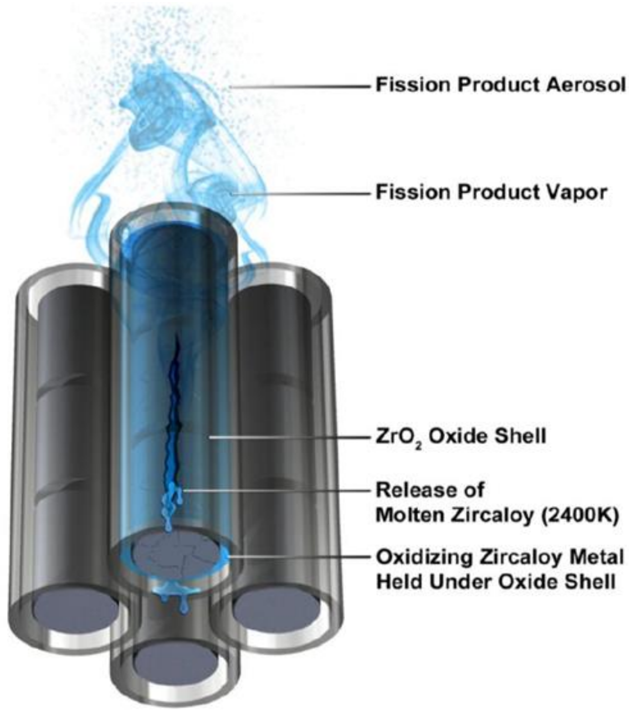

Figure 4. MELCOR Depiction of Fuel Rod Degradation.

This Zircaloy melt breakout temperature represents the uncertain properties that determine the conditions at which oxidized clad mechanically fails, releasing molten unoxidized Zircaloy. This initiates the downward drainage of molten Zircaloy on a ring and axial level basis in the MELCOR simulation. Based on prior work on in-vessel melt progression [33], this parameter is expected to be among the more important uncertain parameters. As described in the previous studies [33], at the "breakout temperature" oxidizing molten Zircaloy is relocated to cooler regions at a time when the oxidation rate is at its peak value. Fuel temperatures are increasing rapidly (~10K/s) at this time, hydrogen generation is locally at a maximum, and fission product release rates are large. The relocation of the oxidizing melt has the effect of terminating the intense local fuel heating, since the chemical heating source has relocated to a cooler region of the vessel. This should affect release rate for volatile fission products and total localized releases of low-volatile species.

The lower bound value is the Zircaloy melting temperature of 2100 K. The value of 2100 K also corresponds to fragile outer oxide shells that are incapable of retaining molten Zircaloy. The upper bound value is based on likely rod collapse temperature occurring within 15 minutes. The upper value of 2540 K, was selected in the original hydrogen uncertainty study [33] based on qualitative consideration of the alpha-Zr(O) phase diagram and observations/analyses of the Phebus experiments [16]-[21]. The mode is the value used in the deterministic SOARCA analysis (Figure 5). The selection of a triangle distribution suggests that a most probable value for the uncertain parameter is recommended (mode), with decreasing likelihood for values away from the most probable. This is in contrast to a range-bounded uniform distribution, where it is implied that any value lying within a range is equally probable

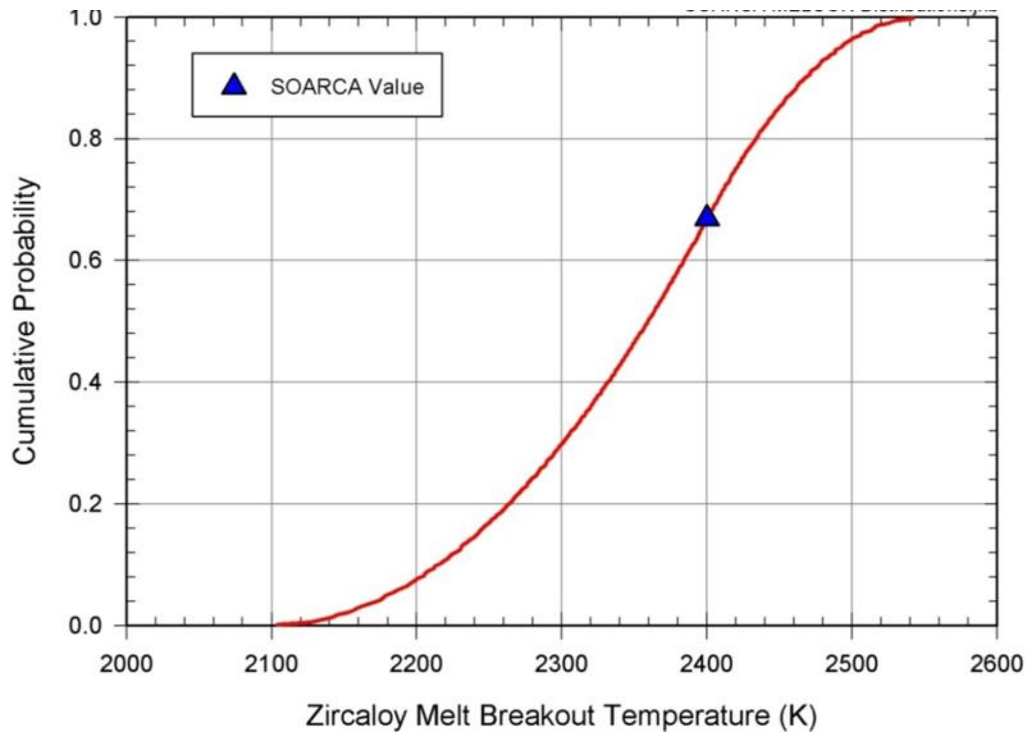

Figure 5. Distribution of Zircaloy Melt Breakout Temperature in the SOARCA UA.

The maximum temperature at which oxidized Zircaloy may support molten Zircaloy metal (SC1131) exhibits a slightly counterintuitive influence on in-vessel accident progression. The earlier (i.e. at lower temperatures) release of molten Zircaloy through the oxidized cladding shell can actually delay core degradation to some extent. This phenomenon is due to the mechanics of the oxidation reactions between zirconium metal and steam. The longer that molten Zircaloy is held up in a region of the core with high temperatures, the more zirconium metal will react and oxidize with steam. And because the zirconium oxidation reaction is exothermic, capable of producing ten times the heat generation rate of the nuclear decay power, allowing the Zircaloy to relocate sooner to cooler regions of the core results in decreased Zirconium oxidation and slower core damage kinetics.

5.1.2 Molten Clad Drainage Rate

The time constant for heat transfer to substrate material versus downward molten flow is highly uncertainty input in MELCOR that influences the in-vessel accident calculations. The molten clad drainage rate impacts material relocation from the top of active fuel to the bottom of active fuel. This parameter (SC1141(2)) represents effective downward flow rate of the molten fuel, balancing heat transfer and freezing on substrate against vertical momentum and, therefore, affects the overall melt progression behavior. It is one of the few MELCOR melt progression parameters available for variation.

A log triangular distribution is used for SC1141(2) with a mode of 0.2 kg/m-s used in the deterministic SOARCA and Fukushima analyses [2][15], and 0.1 and 1.0 kg/m-s respectively for the lower and upper bounds (Figure 6). The selection of a triangular distribution suggests that a most probable value for the uncertain parameter is recommended (mode), with decreasing likelihood for values away from the most probable. The lower and upper bounds of the distribution represent an order of magnitude of uncertainty. This was selected based upon previous studies [33] to ensure the behavior was appropriately captured in the uncertainty in this parameter.

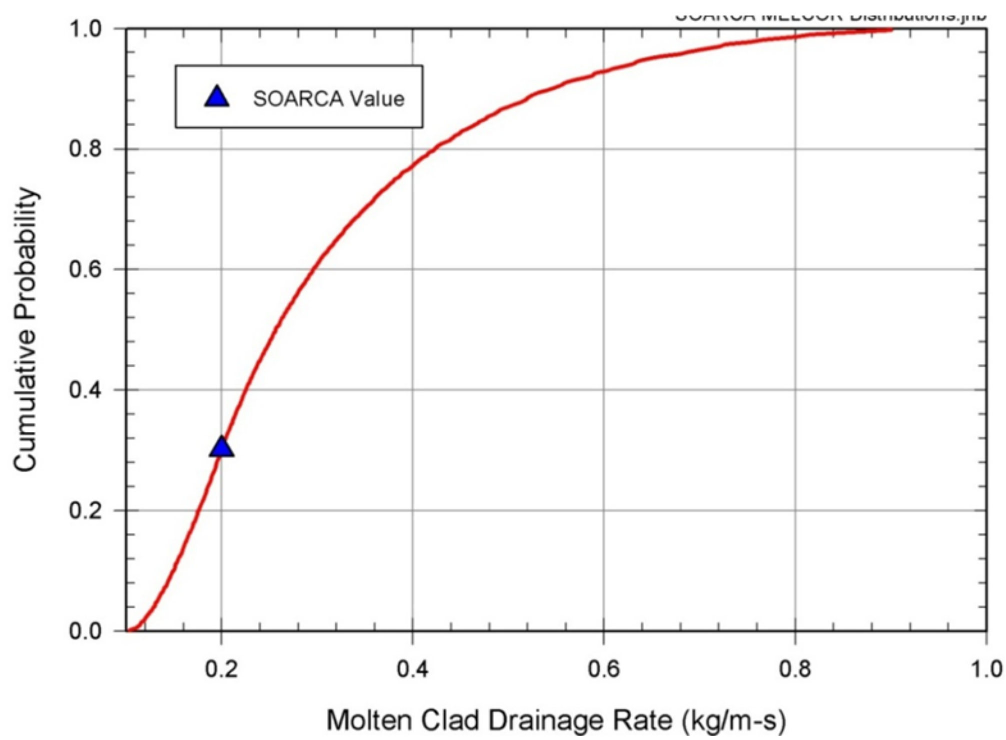

Figure 6. Distribution for Molten Clad Drainage Rate in the SOARCA UA.

5.1.3 Time Constants for Radial Debris Relocation

The time constants for radial relocation of solid and molten debris in the core and lower vessel are highly uncertain parameters. No experimental or high-fidelity computational analyses provide estimates of this information. The Peach Bottom UA project recognized this fact and essentially ‘guessed’ uncertain ranges and distributions for these parameters.

There are two radial relocation models: the first relocates molten core material that still exists following the candling/refreezing process in MELCOR. The second, which relocates particulate debris, is essentially the same algorithm. Both models are intended to simulate the gravitational leveling between adjacent core rings that tends to equalize the hydrostatic head in a fluid medium. Either of the two radial relocation models can be deactivated by user input on MELCOR input record COR_TST, but they are both active by default.

The molten material radial relocation model considers each axial level of the core independently, and is invoked after the axial relocation (candling) model. A simple algorithm loops over all adjacent pairs of radial rings between which relocation is possible and compares the calculated liquid levels in the two. If the levels are unequal, then a calculation is performed to determine the volume of molten material, V_{eq}, which must be moved between the rings to balance the levels. Furthermore, when the stratified molten pool model is active, molten material may reside in both the oxide molten pool component and the metallic molten pool component. Leveling is performed for each component and displacement of metallic molten pool material by assumed heavier oxide molten materials is considered. Furthermore, the non-uniform axial variation of the cell volume for core cells adjacent to the curved lower head is used in determining pool heights. It is assumed that the radial relocation is blocked by the presence of an intact BWR canister structure in either ring. In addition, radial relocation is not allowed within a core plate. The actual implementation prevents such relocation to or from a core cell containing supporting structure modeled as a plate.

The relocation rate has a time constant of τ_{spr}, which may be adjusted by user input, so that the actual volume relocated, V_{rel}, during the COR package timestep, Δt_c, is given by

$$V_{rel} = V_{eq} \left[1 - \exp\left(-\Delta t_c / \tau_{spr}\right)\right]$$

The default value of 60 s for τ_{spr} was chosen as an order-of-magnitude value based on engineering judgment and recommendations of code users. It is accessible as sensitivity coefficient C1020(2) [1].

Radial relocations are directed inward preferentially; that is, at each axial level the algorithm begins at the innermost ring, marches radially outward and transfers molten material from ring i to ring *i*-1 if the liquid level in ring i exceeds that in ring *i*-1. Following the march from ring 1 outward, a reverse march is made inward from the outermost ring to perform any outward relocations from ring *i* to ring *i*+1 still required to achieve a uniform liquid level across the axial level [1].

The radial time constants are MELCOR parameters that influence large scale movement, and are therefore a key parameter in core melt progression. In particular, this parameter can effect debris relocation to the lower plenum following core support failure and slumping. There is no consideration of an angle of repose; debris is completely leveled across the core. Since support failure occurs on a ring-basis, debris previously held in the core in other rings can relocate radially and slump to the lower plenum. The rate of core slumping affects the associated pressure pulse if water exists in the lower plenum. Component volumes and associated fission products are adjusted following relocations.

The distributions are based on expert judgment and are not based on any specific data as no data exists for radial debris relocation. Additionally, the radial debris relocation time constant influences the axial debris relocation. This parameter is qualitative and is a surrogate for more complex relocation processes. Phebus facility tests [16]-[21] offer no insights here as the scale of the testing is too small to provide insights. The parameter ensures that debris does not pile up within single radial rings in an unphysical manner. The exact rate of effective relocation is not known. The values used are felt to bound possible behavior of leveling of materials that may be solid debris, partly molten two phase debris, or fully molten debris.

Exponential time constants for molten debris relocation and solid particulate debris relocation control the rate of relocation of core material. For the uncertainty analysis, a log triangular distribution was selected for both the molten and solid radial relocation time constants. For solid debris, the mode = 360 s, which is the value used in the 'deterministic' SOARCA and Fukushima analyses [2][15], and 180 and 720 s are selected for the lower and upper bounds respectively (Figure 7). A factor of two variation in the 'deterministic' value was used to for the SOARCA-UA work. For molten debris the mode = 60 s, which is the value used in the deterministic SOARCA analysis, and 30 s and 120 s are selected for the lower and upper bounds respectively (Figure 8).

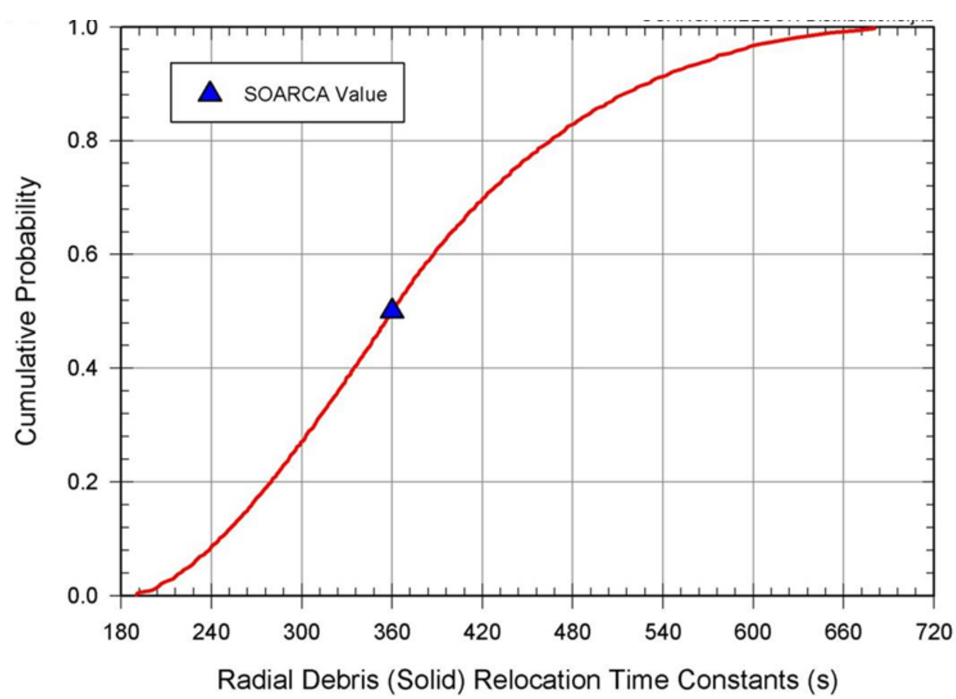

Figure 7. Distribution of Radial Relocation Time Constant for Liquid Debris in the SOARCA UA.

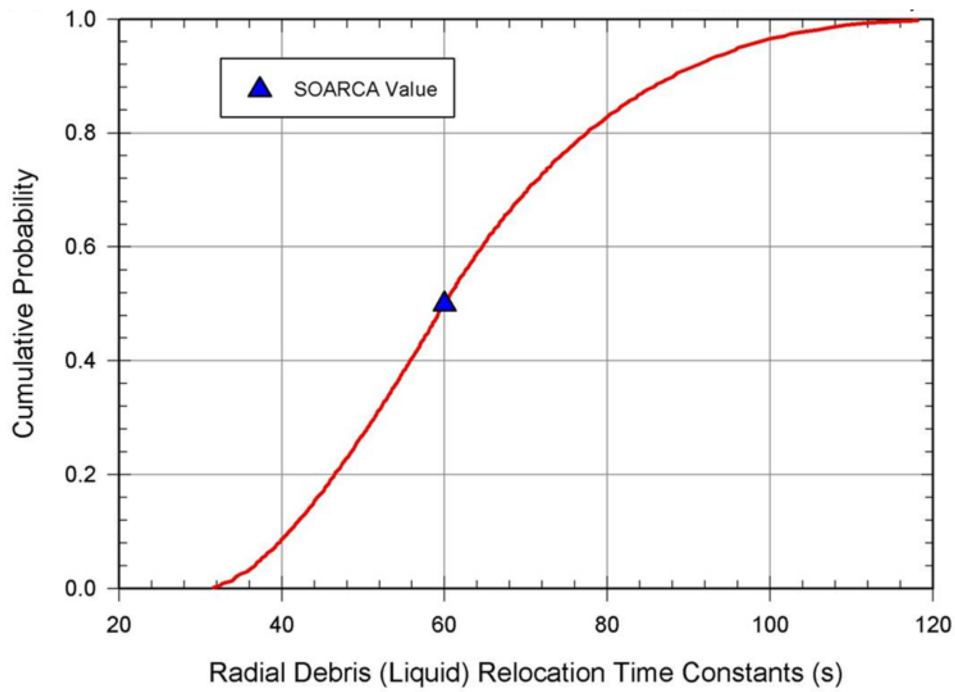

Figure 8. Distribution of Radial Relocation Time Constants for Solid Debris in the SOARCA UA.

5.1.4 Sensitivity Coefficients for MELCOR Models for Core Blockages

There are at least four MELCOR sensitivity coefficients that provide important input for MELCOR modeling of core flow path blockages. Not all of these sensitivity coefficients are in the COR package, and these parameters may need to be correlated in their sampling for uncertainty analysis. The inputs are concerned with minimum debris porosity for flow resistance and heat transfer calculations in the COR package, flow path friction calculations in the MELCOR FL package (Ergun equation), and the minimum hydrodynamic volume fraction that always remains available for hydrodynamic (CVH package) materials no matter the amount of debris occupying the cell. Given the utmost importance of these model input parameters for in-vessel degradation calculations, a more thorough discussion is provided in Section 5.3.

5.1.5 Control Volume Temperature Distribution Models

The dT/dz model is important for capturing heat transfer from multiple (axially stacked) COR cells linked to a single CV, an estimation of the axial temperature profile in the CV atmosphere must be accounted for. Note that most modern MELCOR core models have more axial COR levels than CVH levels. SOARCA has a 2:1 ratio; other MELCOR models may have 1 CVH level for the entire core, while still having 10 or more COR levels. “Approximate local fluid temperatures are calculated for cells above the uppermost liquid level in the core; the remaining cells use control volume pool and atmosphere temperatures." Hence the dT/dz model only plays an important role for COR/CVH cells that are uncovered.

The dT/dz model used for this approximation assumes steady gas flow through the channel or bypass with known or specified inlet gas temperature and no cross-flow between core rings within any single CVH control volume. The model uses time-smoothed ("relaxed") CVH steam and/or oxygen outflow at the top of the core to determine whether the flow direction is upwards or downwards during each COR package subcycle. The flow relaxation time constant is adjustable through sensitivity coefficient C1030(2), which has a default value of 0.1s.

Because fluid temperatures are defined in the CVH package only as volume-averaged quantities and are not defined at particular flow path locations, various methods have been implemented to obtain a suitable inlet temperature for a control volume. The default treatment is to take the inlet temperature as the temperature of the atmosphere flow actually entering the control volume, as calculated by CVH. If the CVH nodalization permits more than one such flow, a heat-capacity-weighted average temperature of the actual inflows is used. If water is boiling in the CVH control volume, the steam generation is treated as an "inflow" at the saturation temperature.

The default treatment will include the effects of cross flows between control volumes representing different radial portions of the core when a detailed CVH nodalization is used. It also minimizes the discrepancies between the calculated dT/dz temperatures and the CVH temperatures. (Note that donor differencing is used in the hydrodynamic equations, so that fluid is advected out of a control volume with enthalpy corresponding to the CVH temperature. For a core volume, this temperature should therefore correspond to the exit temperature for the portion of the core contained in that volume.) Because CVH and COR equations are not solved simultaneously, imperfections in the coupling may result in apparent discontinuities in the profile of dT/dz temperatures between core cells in different CVH volumes. We have found the consequences to be relatively minor, particularly in comparison to the consequences of major discrepancies between dT/dz and CVH temperatures, which cause termination of an execution if a temperature becomes nonphysical.

Once the inlet temperature for a control volume is determined, the temperature at each successive COR cell axial location, moving through the core or lower plenum in the direction of flow, is obtained by performing a simple energy and mass balance. The basic energy balance relates the change in energy in a cell, ΔE_{stored} , during a timestep to the enthalpy flow through the cell, H_{flow} , and any energy sources, q:

$$\Delta E_{stored} + H_{flow} \ \Delta t = q \ \Delta t \tag{1}$$

The terms in Equation (1) are expressed in terms of masses, mass flow rates, and temperatures at the entrance and exit to the cell (note the canceling quantities):

$$\Delta E_{stored} = m^n \ h^n - m^o \ h^o = m^o \ \ c_p \ (T^n - T^o) + (\dot{m}_{in} - \dot{m}_{out}) \ h^n \ \Delta t \tag{2}$$

$$H_{flow} = \dot{m}_{out}\, \mathrm{h}^n - \dot{m}_{in}\, h_{in}^n = \dot{m}_{in}\ c_p\ (T^n - T_{in}^n) - (\dot{m}_{in} - \dot{m}_{out})\ \mathrm{h}^n \tag{3}$$

$$\mathrm{q} = (\mathrm{h^*A})_e\ (T_{s,e} - T_{out}^n) + q_{sou} \tag{4}$$

where

- Δt =timestep,
- m =fluid mass in cell,
- $\dot{m}$ =mass flow rate,
- C_p =gas specific heat,
- h =enthalpy,
- T =cell temperature,
- $(h^*A)_e$ =effective average heat transfer coefficient times surface area for the various cell components in contact with the current CVH control volume,
- $T_{s,e}$ =effective surface temperature for cell components, and
- q_{sou} =source heat rate, from fission product decay heat and B_4C reaction energy deposited in the atmosphere and from heat transfer from heat structures,

and superscripts "*n*" and "*o*" represent new and old time values, respectively.

In the interest of stability, mass flows calculated by CVH are relaxed (smoothed) before use in the previous equations

$$\dot{m}_{dT/dz}^n = \dot{m}_{CVH} + \min\left[\exp\left(-dt/\tau_{RLXZ}\right), f_{\max,old}\right]\left(\dot{m}_{dT/dz}^o - \dot{m}_{CVH}\right) \tag{5}$$

where τ_{RLXZ} is a relaxation time, coded as sensitivity coefficient C1030(2) with a default value of 0.1 s, and $f_{max,old}$ is the maximum permitted weight for the old dT/dz flow, coded as sensitivity coefficient C1030(5) with a default value of 0.6. The use of $f_{max,old}$ is new in MELCOR 1.8.6 and is intended to deal with difficulties encountered when the time scale for flow changes is much less than the relaxation time defined by τ_{RLXZ}.

The dT/dz model in MELCOR 1.8.6 has also been modified to improve coupling between calculations in COR and those in CVH under conditions of little or no flow. The modification involved the assumption that there is a characteristic time for recirculation of fluid *within* each CVH volume, independent of flows *through* the volume, given by sensitivity coefficient C1030(4) with a default value of 10 s. The effect is to add a fraction dt/C1030(4) of the mass in the atmosphere to $\dot{m}_{dT/dz}$ (from eqn. 2.174; note this term is not listed in the eqn. from the reference manual). There are also some interesting notes in the source code concerning SC1030(4):

```
subroutine CORTSV_290
…
!*********************************************************************
!  Add an "internal circulation" term to the inflow to promote coupling
```

```
!  back to CVH temperature under stagnant conditions. The effect is to
!  add a term (YMCPXX*DTC/TAU)*(TVOL(2,ICV)-TGAS) to the right-hand
!  side of the equation, where YMCPXX = cell_share_of_M*Cp/DTC.
!***********************************************************************
! WWWWWWWWWW Error Corrected by V.Belikov, NSI Oct 2005 WWWWWWWWWWWWWWWW
! used before definition - as result changed solution after restart
! see above             FRACT = DTC/C1030(4)
! WWWWWWWWWW Error Corrected by V.Belikov, NSI Oct 2005 WWWWWWWWWWWWWWWW
!             TGAS = TGAS + FRACT*TVOL(2)
!             DEN = (PONE+FRACT)*YMCPXX + XMCPB + SHA
              TGAS0 = TGAS
              FRACT = DTC/C1030(4)
              IF(TVOL(2)>9000.0)THEN
                FRACT=0.8
              ENDIF
              FRACT2=1.
              FRACT2 = 1.-FRACT
              TGAS = TGAS*FRACT2 + FRACT*TVOL(2)
              DEN = (FRACT+FRACT2)*YMCPXX + XMCPB + SHA
              DEN2= (FRACT+FRACT2)*YMCPXX + XMCPB + SHAAst(IA,IR) +SHA
              Adder=0.0
…
end subroutine CORTSV_290
```

The model solves for the value of T^n, which is then used as T_{in}^n for the next higher cell. Control volume average values for mass and mass flow rates are currently used at the inlet to the control volume and are updated for the effects of oxidation for each cell. For multiple core rings within the same control volume, the inlet mass flow rate is multiplied by the fraction of the total flow area for each ring, thus partitioning the flow across all rings.

For the dT/dz model to function correctly and model the phenomena appropriately, it is important that the heat structures representing the radial core boundary (e.g., core shroud) communicate with the fluid temperatures calculated by this model. The outer ring core cells must be specified as the fluid temperature boundary on input record HS_LBF/HS_RBF (see the HS Package Users' Guide) unless the IHSDT option switch provided on input record COR_MS has been set to 1.

The heat transfer rates obtained by using the dT/dz temperatures in conjunction with the core component surface areas and temperatures in all of the core cells associated with each CVH control volume within the core are summed and compared to the value which would be obtained if the CVH vapor temperature in that volume had been used instead of the dT/dz temperatures. If the heat transfer rates thus obtained are of opposite sign, then it is assumed that the dT/dz model is malfunctioning (probably because prevailing conditions are outside the scope of its intended application) and the dT/dz temperatures are overwritten by relaxing their beginning-of-step values with the value of the CVH vapor temperature in the corresponding CVH volume. Hence, if the model is malfunctioning, then relaxed CVH vapor temperatures are used instead, and the relaxation time constant for the CVH temperatures is adjustable through sensitivity coefficient C1030(3). Also, if the dT/dz model is deactivated by user input, then relaxed CVH temperatures are always used in place of results from the deactivated model.

SENSITIVITY COEFFICIENT FOR dT/dz MODEL

1030 – dT/dz Model Parameters

1. Option switch (default = revert to treatment used in MELCOR 1.8.3)
2. Time constant for averaging flows (default = 0.1 sec)
3. Time constant for relaxing dT/dz temperatures towards CVH volume temperature when dT/dz model is disables (default = 1.0 sec)
4. Characteristic time for coupling dT/dz temperatures to average CVH volume temperature when dT/dz model is active (default = 10 sec). This parameter is used to improve coupling between COR and CVH for near stagnant flow, and essentially assumes a characteristic time for recirculation flow within a CV that is independent of flow through the CV. Effectively this model increases the mass flow rate for dT/dz model. This is an important and highly uncertain parameter that has a strong effect on code performance (i.e. error avoidance) and results for the slower-progressing accidents like unit 2 and unit 3, especially with core injection and re-flood of a partially degraded core. The MELCOR reference manual describes the details of SC1030(4).
5. Maximum relative weight of old flow in smoothing algorithm involving time constant for averaging flows (default = 0.6)

Reverting to the dT/dz treatment used in MELCOR 1.8.3 is part of the current best-practices. It was decided to not vary this treatment and instead focus on the effect of dT/dz model parameter variation.

Since the dT/dz model is on, sensitivity coefficient value 3 is not applicable.

For the Fukushima UA, the following sensitivity coefficient values will be sampled:

- Time constant for averaging flows
  uniform distribution; LB = 0.09 s; UB = 0.11 s
- Characteristic time for coupling dT/dz temperatures to average CVH volume temperature when dT/dz model is active
  uniform distribution; LB = 9 s; UB = 11 s
- Maximum relative weight of old flow in smoothing algorithm involving time constant for averaging flows
  uniform distribution; LB = 0.54 s; UB = 0.66 s

The uncertainty for these parameters was chosen to be uniform and varying by +/- 10% around the default value. This treatment is sufficient to examine the effect of their variation on model results.

5.1.6 RPV Lower Head Failure

Parameter variations that affect in-vessel accident progression drive associated changes in the prediction and timing of RPV lower head failure. Uncertainties related to early accident sequence boundary conditions and to physics model inputs for the COR package alter the rate of debris relocation to the lower plenum, the heat generation in the debris bed, the initial temperature of the debris, and the initial liquid water inventory in the lower plenum; such variations can change the timing of lower head failure by several hours [5][15]. Hence, previous MELCOR uncertainty studies assumed the inherent variability of the timing of lower head failure subsumed any uncertainties in the lower head model itself. This approach is reasonable for accident scenarios that always result in lower head failure. In the Fukushima accident scenarios, however, it is still uncertain as to whether RPV lower head failure actually occurred, given partial success of operator mitigation actions (e.g. core injection and containment sprays). Therefore, the prediction, extent, and timing of lower head failure is much more ambiguous for the Fukushima reactors; this calls for more detailed analyses into the uncertainties associated with simulating lower head failure using simplified models in engineering-level codes such as MELCOR.

The Fukushima UA can examine uncertainties in key sensitivities coefficients, such as the strain value to initiate gross failure (default = 18% given by SC1601(4)), uncertainties in material properties, and computational uncertainties associated with the lower head mesh. In MELCOR the lower head can be treated as a hemisphere or a truncated hemisphere. The surface of the lower head is a coarse 2D mesh comprised of segments and through-wall nodes (Figure 9).

Uncertain parameter distributions and ranges can be informed by the lower head failure experimental program performed at SNL [37]. Additional uncertainties related to geometric/material discontinuities such as lower head penetrations are outside the scope of MELCOR’s capabilities and thus will not be considered in the Fukushima UA. Also, corrosion effects due to seawater injection must be neglected, which is likely reasonable assuming lower head failure occurred soon into the accident–the timescales of significant corrosion effects are typically longer than severe accidents (1-4 days).

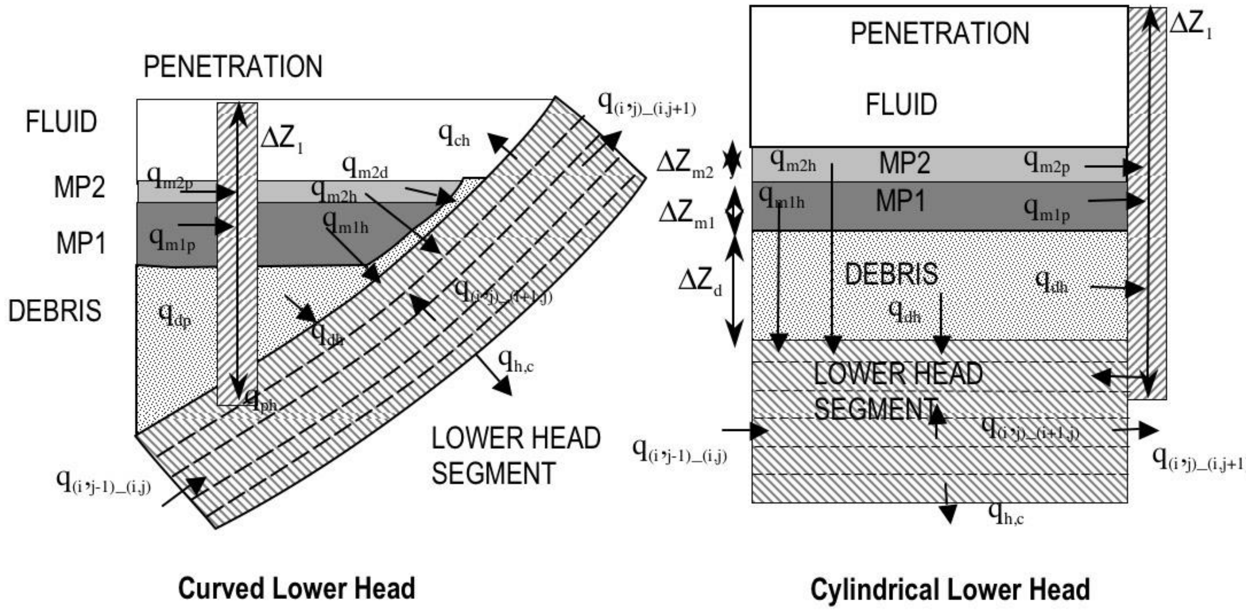

Figure 9. Lower head mesh nodalization and heat transfer. The whole lower head is comprised of several such segments, each containing several through-wall nodes.

The lower head mesh may be finer than corresponding/linked COR nodalization. That is, "for MELCOR 1.8.6 and 2.0, heat transfer is calculated for each lower head segment (rather than ring), for which multiple segments may intersect with a single-core cell," and "MELCOR 1.8.6 and 2.0 allow the specifications for multiple segments to interface with a COR cell to allow a more detailed calculation of the temperature profile in the lower head." However, a LH segment may not communicant with *multiple* COR cells, i.e. the LH mesh may not be coarser than the corresponding/linked COR nodalization. In other words, a LH segment interface must exist for every COR ring/level intersection with the LH surface.

<u>LH failure algorithm:</u>

- Lower head failure occurs at 18% strain by default, i.e. SC1601(4)
- Larson-Miller models provides a time-to-rupture, which is used in a cumulative strain equation

$$\varepsilon_{pl}(t+\Delta t) = \varepsilon_{pl}(t) + SC1601(4)\frac{\Delta t}{t_R}$$, plastic strain (eq. 6.25)

- In the strain equation, the time-to-rupture, t_R, is given by:

$$t_R = 10^{\left(\frac{P_{LM}}{T} - C1601(3)\right)}$$, time to rupture (eq. 6.23)

- The Larson-Miller parameter (P_{LM}) depends on stress and is given by:

$$P_{LM} = 4.812x10^4 - 4.725x10^3 \quad \log_{10} \sigma_e$$ (eq. 6.24)

The constants above are SC1601(1) and SC1602(2): $P_{LM} = C1601(1) \cdot \log_{10} \sigma_e + C1601(2)$

The *effective stress* in the Larson-Miller parameter is calculated by 2D temperature (elastic modulus and yield stress are functions of temperature, and thermal strain is included) and 1D stress distributions across the lower head. A zero dimensional stress model option is also available but is not best practice. Here's the one-dimensional stress algorithm:

The one-dimensional model requires that the stress distribution integrated over the vessel thickness be equal to the imposed load:

$$[\,\Delta P + \rho_d \, g \, \Delta z_d\,]\, R_0^2 = \sum_{i}^{N_{NY}} \sigma_i \left(R_i^2 - R_{i-1}^2 \right) + \sum_{j}^{N_Y} \sigma_Y \left(T_j\right) \left(R_j^2 - R_{j-1}^2 \right)$$, stress balance (eq. 6.29)

(ΔP is the pressure difference across the lower head, ρ_d and Δz_d are the density and depth of the debris resting on the lower head).

The first sum on the right-hand side is over all layers that have not yielded, N_{NY}, and the second sum is over all layers that have yielded, N_Y. The stress, σ_i, in layers that have not yielded is given by

$$\sigma_i = E(T_i) \left[\varepsilon_{tot} - (\varepsilon_{pl,i} + \varepsilon_{th,i}) \right]$$, for layers that have not yielded (eq. 6.30)

where $E(T_i)$ is the value of the elastic modulus at the average temperature in mesh layer *i*, which is equal to the average of the node temperatures on the two boundaries, ε_{tot} is the total strain across the lower head for that particular segment, which is the same for mesh layers in that segment, and $\varepsilon_{pl,i}$ and $\varepsilon_{th,i}$ are the plastic and thermal strains, respectively, in mesh layer *i*. The thermal strain is given by

$$\varepsilon_{th,i} = C1600(2)\left(T_i - T_{ref}\right)$$, thermal strain known from temperature profile (eq. 6.31)

$$E(T) = C1602(1) \left[\frac{1}{1 + \left(\frac{T}{C1602(3)} \right)^{C1602(4)}} - \frac{1}{1 + \left(\frac{C1602(2)}{C1602(3)} \right)^{C1602(4)}} \right]$$, elastic modulus (eq. 6.27)

$$\sigma_Y(\mathrm{T}) = C1603(1)\left[\frac{1}{1+\left(\frac{\mathrm{T}}{C1603(3)}\right)^{C1603(4)}} - \frac{1}{1+\left(\frac{C1603(2)}{C1603(3)}\right)^{C1603(4)}}\right]$$, yield stress (eq. 6.28)

Equations 6.29 and 6.30 are solved implicitly and iteratively for ε_{tot}, σ_i, and $\varepsilon_{pl,i}$ ($\varepsilon_{th,i}$ is known because the temperature profile is known) using Equations 6.23 – 6.25 to update the plastic strain profile with the latest stress profile after each iteration. Failure is declared when ε_{tot} reaches 18% (the use of ε_{tot} rather than ε_{pl} makes little difference because the elastic and thermal strains are insignificant compared to the plastic strain when ε_{tot} becomes large).

<u>Sensitivity Coefficients for RPV Lower Head Failure</u>

1600 – Model Parameters

(1) Switch to choose zero-dimensional (0.0) or one-dimensional (1.0) modeling of the stress and strain distribution in the lower head.
(default = 1.0, units = none, equiv = none)

(2) Linear expansivity of the lower-head-load-bearing material. (Note, this value is only used if the one-dimensional model has been selected.)
(default = 1.E-5, units = K^{-1}, equiv = none)

(3) Differential pressure lower limit. The mechanical model will be bypassed whenever the effective differential pressure across the lower head falls below this value. Hence, a large value for this coefficient (e.g., 1.E10) will totally disable the mechanical model.
(default = 1.E3, units = Pa, equiv = none)

1601 – Larson-Miller Creep Rupture Parameters for Vessel Steel

(1) Inherently negative multiplicative constant.
(default = -4.725E3, units = none, equiv = none)

(2) Inherently positive additive constant.
(default = 4.812E4, units = none, equiv = none)

(3) Additive exponential constant.
(default = 7.042, units = none, equiv = none)

(4) Total strain assumed to cause failure.
(default = 0.18, units = none, equiv = none)

1602 – Vessel Steel Elastic Modulus Parameters

(1) Leading multiplicative constant.
(default = 2.E11, units = Pa, equiv = none)

(2) Temperature at which elastic modulus vanishes.
(default = 1800.0, units = K, equiv = none)

(3) Temperature at which elastic modulus is approximately halved.
(default = 900.0, units = K, equiv = none)

(4) Exponent of scaled temperatures.
(default = 6.0, units = none, equiv = none)

1603 – Vessel Steel Yield Stress Parameters

(1) Leading multiplicative constant.

(default = 4.E8, units = Pa, equiv = none)

(2) Temperature at which yield stress vanishes.
(default = 1700.0, units = K, equiv = none)

(3) Temperature at which yield stress is approximately halved.
(default = 900.0, units = K, equiv = none)

(4) Exponent of scaled temperatures.
(default = 6.0, units = none, equiv = none)

1604 – Larson-Miller Creep Rupture Parameters for Supporting Structure

- Default values are typical for stainless steel

1605 – Internal Steel Elastic Modulus Parameters – for supporting structures

1606 – Internal Steel Yield Stress Parameters– for supporting structures

The model for lower head failure has a large number of sensitivity coefficient values. Rather than look at the uncertainty in all of them, only the total strain assumed to cause failure will be evaluated in this analysis. This parameter has a direct, linear effect on the time of lower head failure. As such it can act as an acceptable surrogate for the larger set of parameters to address the issue of uncertainty in lower head failure timing.

The uncertainty for this parameter was chosen to be uniform and varying by +/- 10% around the default value. This treatment is sufficient to examine the effect of its variation on model results.

5.2 Additional Uncertain COR Package Input

Other uncertain model input exists in the COR package that are not currently available as sensitivity coefficients. Some of these inputs were identified as important uncertain parameters for the Fukushima UA and are discussed in this section

5.2.1 Thermal-Mechanical Weakening of Oxidized Cladding

Zircaloy cladding reacts with steam to form outer oxide shells. The oxide shells would have a high melting temperature relative to that of unoxidized cladding and, as evidenced in the Phebus experiments, would maintain fuel geometry as Zircaloy interior to the shell melted and drained away (see Section 5.1.1) [1][15].

Thermal-mechanical weakening of oxidized rods may be especially important for Fukushima accidents. Compared to Peach Bottom SOARCA, the Fukushima reactors have lower decay powers, smaller cores, and less metal available for oxidation reactions, especially 1F1.

The oxide shells supporting the fuel rod geometry are susceptible to thermal-mechanical weakening over time. The rod collapse model in MELCOR acknowledges this thermal-mechanical weakening as a function of time and temperature. Fractional damage in this model is accrued locally by axial level and radial ring throughout the core. Damage accumulation begins once unoxidized (metal) cladding thickness drops below 10% of nominal values. However, this model is not active by default in MELCOR input. The user must manually add the COR_ROD input record and specify the time-versus-temperature tabular function, as well as the absolute unoxidized cladding thickness at which to begin the time-at-temperature treatment of fuel rod collapse. Without this model active, an oxide shell could maintain fuel geometry at very high temperatures for a long period of time after interior Zircaloy drained away (ending oxidation and the associated heat generation). The oxide shell would not fail until its temperature reached the eutectic temperature for the UO_2/ZrO_2 system (2500 K), and with oxidation heat generation gone this could take a long time. The Rod Collapse Model eliminates this threshold effect of the default temperature requirement failure for rod collapse [1][15]. The best-practice dependence of time-to-failure as a function of temperature is presented in Table 5.

Table 5. Best-Estimate Time to Fuel Rod Collapse versus Cladding Oxide Temperature.

Oxide temperature	Time to Failure
2000 K	Infinite
2090 K	10 days
2100 K	10 hours
2500 K	1 hour
2600 K	5 min
2700 K	30 sec

The values in Table 5 are linearly interpolated. Infinite lifetime is assumed at cladding oxide temperatures below the melting point of Zircaloy. The short times to failure associated with 2500 K and 2600 K reflect the observations of irradiated fuel relocation in the Phebus experiments [16].

Uncertainty in time-to-failure as a function of temperature is being evaluated as part of the on-going Surry uncertainty analysis. In that analysis, the current thinking is to select from three characterizations time-to-failure as a function of temperature, where each characterization has an equal weight.

- SOARCA best-estimate (Table 5)
- 2x SOARCA best-estimate times-to-failure
- 0.5x SOARCA best-estimate times-to-failure

Figure 10 shows a plot of the three characterizations.

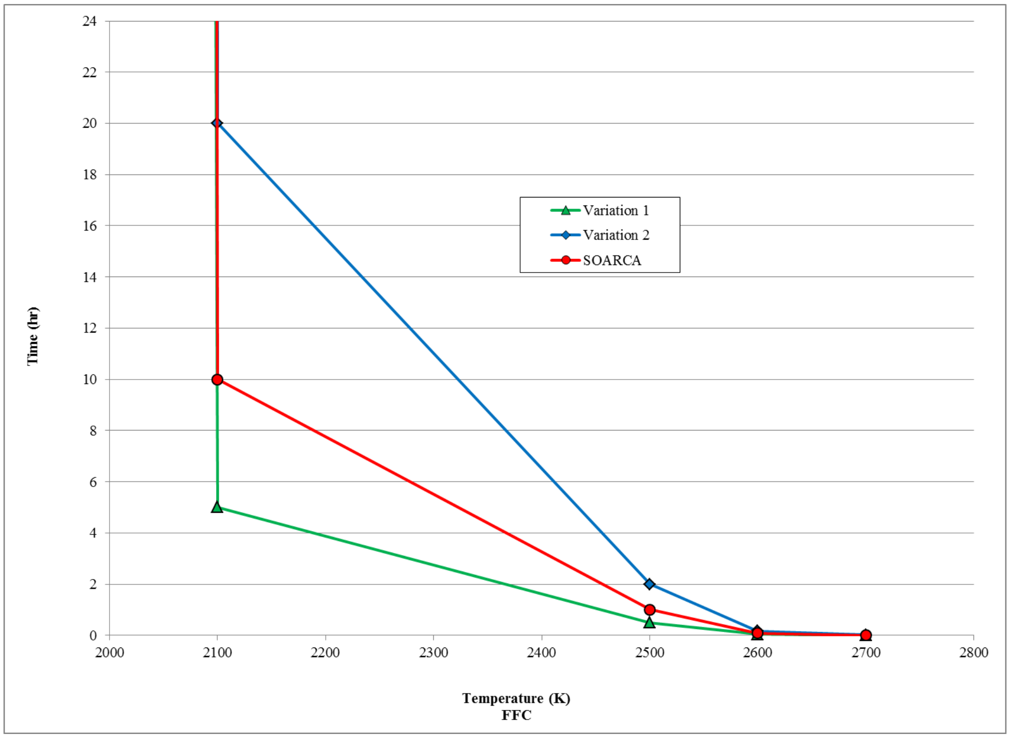

Figure 10. Proposed characterizations of time-to-failure as a function of temperature for the Surry uncertainty analysis (each curve has equal weight).

The Fukushima uncertainty analysis will use a variation of what is being proposed for the Surry UA; the uncertainty in time-to-failure as a function of temperature will be treated as varying uniformly between +/- 50% of the SOARCA best-estimate times-to-failure values (see Figure 11).

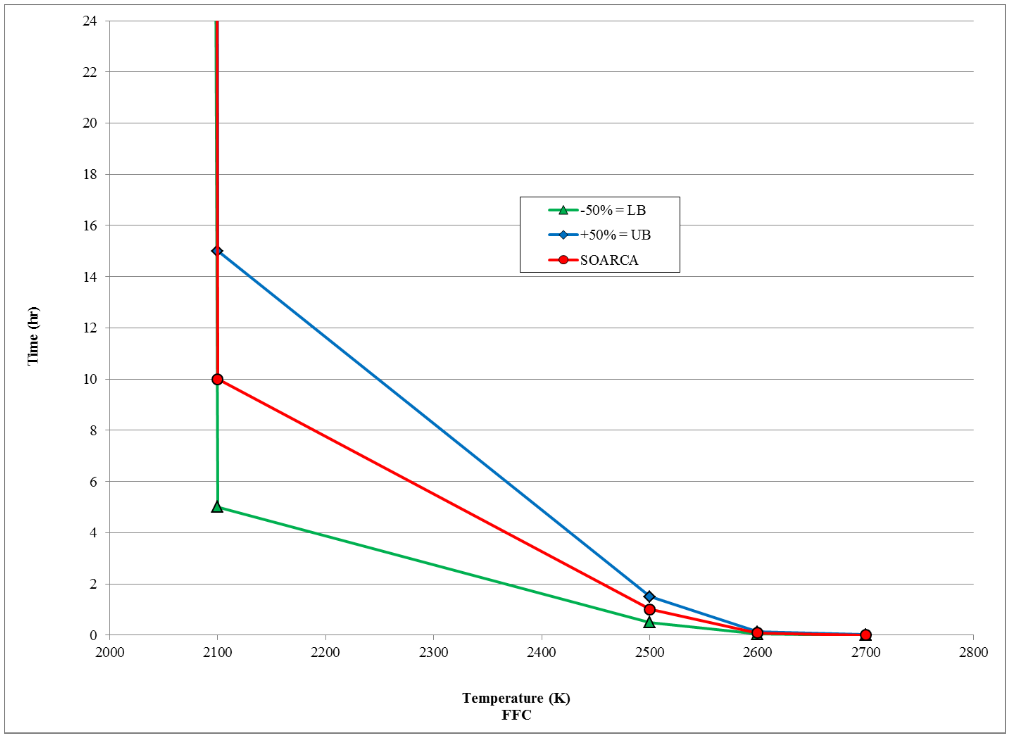

Figure 11. Characterizations of time-to-failure as a function of temperature for the Fukushima uncertainty analysis (uniform uncertainty between the lower and upper bound).

5.2.2 Candling Secondary Material Transport Parameters

The uncertainty in the candling model refreezing heat transfer coefficients will be treated as being indicative of the uncertainty in how readily material refreezes, hence the parameters will be treated as being perfectly correlated. They will be sampled uniformly between +/-10% of their default values. This treatment is sufficient to examine the effect of their variation on model results.

The material candling transport parameters are specified on the COR_CHT record. These parameters determine the refreezing heat transfer coefficients to be used in the candling model for each of the molten core materials. Each value must be positive. Due to a large degree of phenomenological uncertainty, it is very difficult to justify particular values for these coefficients. The default values are order-of-magnitude estimates that appear to produce plausible simulations of relocation phenomena, but they should be varied in sensitivity studies to determine their impact on overall melt progression behavior. For more information on how these quantities are used in the candling model, see the MELCOR COR Package Reference Manual, Section 3.1 [1].

```
! ---------------------------------------------
! candling heat transfer coefficients (defaults)
! ---------------------------------------------
COR_CHT  7500.0  7500.0  7500.0  2500.0  2500.0  2500.0
```

(1) HFRZZR
   Refreezing heat transfer coefficient for Zircaloy.
   (type = real, default = 7500.0, units = W/m^2-K)

(2) HFRZZX
   Refreezing heat transfer coefficient for ZrO_2.
   (type = real, default = 7500.0, units = W/m^2-K)

(3) HFRZUO
   Refreezing heat transfer coefficient for UO_2.
   (type = real, default = 7500.0, units = W/m^2-K)

(4) HFRZSS
   Refreezing heat transfer coefficient for steel.
   (type = real, default = 2500.0, units = W/m^2-K)

(5) HFRZSX
   Refreezing heat transfer coefficient for steel oxide.
   (type = real, default = 2500.0, units = W/m^2-K)

(6) HFRZCP
   Refreezing heat transfer coefficient for the control poison material.
   (type = real, default = 2500.0, units = W/m^2-K)

The uncertainty in the candling model refreezing heat transfer coefficients will treated as being indicative of the uncertainty in how readily material refreezes, hence the parameters will be treated as being perfectly correlated. They will be sampled uniformly between +/-10% of their default values. This treatment is sufficient to examine the effect of their variation on model results.

5.2.3 Lipinski Dryout Model of a Submerged Debris Bed

After severe core damage and relocation following support failure (slumping), core debris is hypothesized to exist as a debris bed in the RPV lower plenum. The Lipinski Dryout Model simulates the reduced coolability of this debris bed given the loss of channel/assembly geometry. In one-dimensional form, the model is derived from mass, momentum, and energy balance equations, where momentum equations for liquid and vapor are based on Ergun formulas that relate laminar flow, turbulent flow, and pressure drop for porous media [38][39]. The model incorporates the effects of two-phase friction, capillary forces, gravitational head, and channels leading into the top of the debris bed. The basic form of the one-dimensional Lipinski model is ultimately a first order differential equation [39].

For faster computation in PRA codes with 1980s computing capabilities, MELCOR incorporates the simplified zero-dimensional Lipinski correlation. A simplified interpretation of the correlation is that it represents liquid flowing down into the debris bed and vapor flowing upward, thereby inhibiting further liquid flow into the debris bed. The differential equation for the one-dimensional Lipinski model is reduced to an algebraic equation using the following approximations [39]:

1. The debris bed thickness is much greater than the capillary head (i.e. the deep-bed approximation).
2. Surface tension in the differential equation is zero (note that surface tension term is still treated in the accounting of capillary head).
3. Capillary forces are treated approximately and added to the hydrostatic head.
4. The debris bed is uniform (i.e., no debris stratification)

The Lipinski zero-dimensional correlation ultimately yields an estimated dryout heat flux, which reflects the maximum rate of heat removal from the debris bed. In MELCOR nodalization schemes for the lower RPV, total heat transfer rates are determined at each axial level in the lower plenum. The highest axial level is determined that has total heat transfer rates equal to or greater than the maximum rate estimated by the Lipinski model; all heat transfer below this axial level is neglected for debris and intact lower structures [1].

The 16^{th} record on the COR_TST input is used to activate or deactivate the model. Deactivating the model essentially assumes perfect coolability of the debris bed, which acts to prevent lower head failure until the lower plenum is nearly void of liquid water. The default MELCOR treatment in recent years, such as in the SOARCA studies [13], has been to deactivate the model. For the Fukushima UA the activation and deactivation of the model will be considered, as well as the associated uncertainty in the model's parameters on sensitivity coefficient 1244 [1].

SC1244 - Debris Dryout Heat Flux Correlation: These coefficients are used to calculate the dryout heat flux for particulate debris beds using the zero-dimensional Lipinski turbulent correlation, given in Section 2.3.7 of the MELCOR COR Package Reference Manual [1]

1. Leading coefficient, default = 0.756, units = none

2. Capillary head for water and 0.5 mm particles, default = 0.089, units = m
3. Minimum debris porosity allowed, default = 0.15, units = none

The COR package uses the Lipinski zero-dimensional correlation to calculate the dryout heat flux, q_d, which is then applied as a limiting maximum heat transfer rate from a particulate debris bed (using the cell cross-sectional area rather than the total particulate surface area), which may occupy one or more axial levels:

$$q_d = 0.756\ h_{lv} \left[\frac{\rho_v\ (\rho_l - \rho_v)\ g\ d\varepsilon^3\ (1 + \lambda_c / L)}{(1-\varepsilon)\ \left[1 + (\rho_v / \rho_l)^{1/4}\right]^4} \right]^{1/2} \tag{6}$$

In this equation, h_{lv}, ρ_l, and ρ_v are the latent heat, liquid, and vapor densities of water, respectively; g is the gravitational acceleration; d is the debris particle diameter; ε is the bed porosity; L is the total bed depth; and λ_c is the liquid capillary head in the debris bed,

$$\lambda_c = \frac{6\ \sigma\ \cos\theta\ (1-\varepsilon)}{\varepsilon\ d\ (\rho_l - \rho_v)\ g} \tag{7}$$

where σ is the water surface tension and θ is wetting angle. The leading constant, the nominal capillary head for 0.5 mm particles in approximately 0.089 m of water, and the minimum bed porosity allowed in the correlation are accessible to the user as sensitivity coefficient array C1244. A default minimum porosity of 0.15 was selected to ensure that some heat transfer occurs from molten debris pools. The actual capillary head is adjusted for particle diameter size within the model.

In the Fukushima UA, the Lipinski dryout model will be activated and its minimum debris porosity will be varied uniformly with a lower bound of 0.01 and an upper bound of 0.2. These values were chosen to span the default value of 0.15 and to be consistent with the debris porosity used in the blockage model (see Section 5.3).

5.2.4 Debris Quenching Input

Large-scale relocation of core material to the lower plenum occurs following gross core damage and support failure. Depending on the boundary conditions for the accident scenario, the lower plenum may still contain a substantial quantity of liquid water. MELCOR models the quenching of hot core debris falling into this water pool and has best practice model parameters based on the FARO experiments. These model parameters are uncertain and have first-order impacts on the thermal-hydraulic responses in the RPV and containment after core slumping, which usually manifests as large and rapid peaks in pressure signatures. The debris quenching model also affects the initial temperature response of debris in the lower plenum, and is therefore important for the subsequent calculations of RPV lower head response.

The falling-debris quench model can be activated/deactivated by changing the heat transfer coefficient (‘HDBH2O’, a value of 0.0 deactivates it) on COR_LP.

```
!      ia,supportPlate   coeff to pool   dP for LH fail   v,falling debris
COR_LP  4                  2000.0         2.0E7             0.01
```

The model calculates heat transfer from the debris to the pool based on the used-selected debri-to-pool heat transfer coefficient and the debris falling velocity. The MELCOR code defaults are 100 W/m^2-K and 1.0 m/s, respectively, while the current best-practices values used in SOARCA are 2000 W/m^2-K and 0.01 m/s, respectively.

For the Fukushima UA, the uncertainty in these parameters will be characterized by using the MELCOR code default and SOARCA values as lower and upper bounds, as appropriate. A log-uniform distribution will be used for both parameters to ensure uniform sampling over the orders-of-magnitude spanned by the distributions.

5.3 Treatment of Core Blockages

MELCOR modeling of flow blockages due to core material relocation depends on the COR, CVH, and FL nodalization of the core and lower plenum regions. All core and lower vessel flow paths that are connected to lower plate region, active core region, and upper core/plate region should have blockage (FL_BLK) input specified. In the SOARCA models these regions are finely nodalized with several COR, CVH, and FL connections; hence material relocation can fill a relatively small volume (e.g. bypass volume) and create difficulties for MELCOR thermal-hydraulics; hence variation of core blockage inputs can result in larger differences in code CPU time and success. The UA will vary these inputs to quantify the effects that relatively small differences in initial and late core blockages have on in-vessel accident progression, which can subsequently affect later stages of the accident.

MELCOR treats the entire range of degradation from partially blocked rod geometry to debris bed geometry. The markedly increased resistance to flow in severely degraded geometries is particularly important because it limits the flow available to carry away decay heat and to provide steam for core oxidation. In addition to improving the basic modeling, inclusion of blockage effects has been found to improve code performance, particularly when a detailed CVH nodalization is used in the core region. The neglect of blockage can lead to prediction of non-physical large flows through regions containing very little fluid; the material Courant condition will then force extremely small timesteps, greatly increasing execution times.

Relocation of core materials may result in a reduction of area and an increase of flow resistance, or even a total blocking of flow, within various parts of the core. The effects on hydrodynamic flows may be modeled by using the core flow blockage model in the hydrodynamics package, which requires input of FL_BLK records for the associated flow paths. In addition to modeling the change in flow area, this model calculates the change in flow resistance. The resistance is based on a model for flow through porous media when particulate debris is present; otherwise, the input flow resistance for intact geometry is simply modified to account for any change in flow area. Activation of these models is not automatic. Input on FL_BLK records is required to specify which core cells are associated with each flow path involving the core. Furthermore, because only CVH and FL model the flow of water and gases, the effects of blockages on circulation can be modeled only to the extent that the CVH/FL nodalization can resolve that circulation.

The current model considers two flow regimes. For severely damaged core geometries, after particulate debris has been formed, it uses correlations developed for flow in porous media. Until this occurs, a simple modification to the flow resistance in intact geometry is used to account for changes in flow area associated with refrozen conglomerate debris. As currently coded, the switch in regimes is made on a flow path by flow path basis, triggered by the first appearance of particulate debris in any core cell associated with the flow path. When the uncertainty in predicting the actual geometry of core debris is considered, we believe that this simple treatment is adequate for MELCOR use.

<u>Important Inputs for MELCOR Flow Blockage Modeling in the Core and Vessel:</u>

- COR, FL, and CVH nodalization (see Figure 12).
- For the Fukushima models, treatment of flow path blockages from the lower plenum to the core (core inlet) across the core plate was found to be particularly important. Debris accumulates on the plate and the cells above the plate, displacing CVH volume in the lower channels volumes, bypass volumes, and lower plenum.

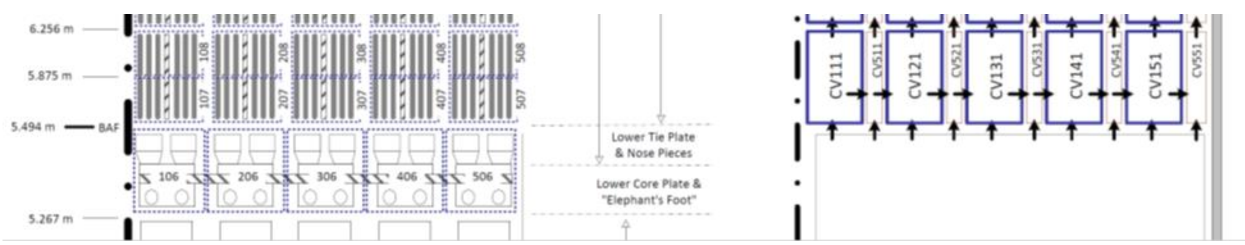

Figure 12. COR, FL, and CVH Nodalization for Lower Core and Core Plate.

- FL_BLK input:

  (1) OPTION

  Flow geometry to be modeled in this path.

  (a) AXIAL

  - Axial flow geometry. May be used for a BWR only if the channel and bypass are not distinguished in any of the core cells involved.

  AXIAL-C

  - Axial flow geometry. Used for a BWR or the peripheral region of a PWR.

AXIAL-B

- Axial flow geometry, considering only the bypass region for a BWR.

RADIAL

- Radial flow geometry. Not recommended for a BWR because the channel and bypass regions are treated as combined

RADIAL-C

- Radial flow geometry, considering only the channel region. Used for paths connecting to the peripheral region of a PWR.

RADIAL-B

- Radial flow geometry, considering only the bypass region for a BWR.

CHANNEL-BOX

- Connection between channel and bypass of a BWR that opens when the channel box fails.

CORE-SHROUD

- Connection between channel and bypass in the peripheral region of a PWR that opens when the core shroud (baffle) fails.

(2) ICORCR1 (3) ICORCR2

Define the limiting core rings to be associated with the flow by defining two corner core cells. Each core cell in the range must be associated with either the "From" or the "To" control volume for the flow path as defined on the FL_FT record.
(type = integer, default = none, units = dimensionless)

(4) ICORCA1 (5) ICORCA2

Define the limiting core axial levels to be associated with the flow path by defining two corner core cells. Each core cell in the range must be associated with either the "From" or the "To" control volume for the flow path as defined on the FL_FT record.
(type = integer, default = none, units = dimensionless)

(6) FLMPTY

Form loss coefficient for empty geometry to be added to the value from the Ergun correlation.
Optional.
(type = real, default = 1.0, units = dimensionless)

COR Package Sensitivity Coefficients Related to Blockage Modeling:

- 1505 - These coefficients specify the geometric parameters affecting core flow resistance and heat transfer under conditions of flow blockage.

1. Minimum porosity to be used in calculating the flow resistance in the flow blockage model. Default = 0.05. PB SOARCA value = 0.05
2. Minimum porosity to be used in calculating the area for heat transfer to fluid. Default = 0.05. PB SOARCA value = 0.05

CVH/FL Package Sensitivity Coefficients Related to Blockage Modeling:

- 4413 - Flow Blockage Friction Parameters: These parameters are used to calculate the friction loss in a flow path that has been at least partially blocked by debris. The pressure drop will be based on a generalized Ergun equation in the form

$$K_{eff} = \left[C4413(1) + C4413(2)\left(\frac{1-\varepsilon}{\mathrm{Re}}\right) + C4413(3)\left(\frac{1-\varepsilon}{\mathrm{Re}}\right)^{C4413(4)} \right] \frac{(1-\varepsilon)\,L}{\varepsilon\, D}$$

  where ε is the porosity and D is the particle diameter, and $\mathrm{Re} = \rho j D / \mu$ is the Reynolds number based on the superficial velocity (volumetric flux) j, the fluid viscosity μ, and the particle diameter.

  (1) Coefficient of the turbulent term in the generalized Ergun equation.
  (default = 3.5, units = dimensionless, equiv = CTERG)
  (2) Coefficient of the laminar term in the generalized Ergun equation.
  (default = 300.0, units = dimensionless, equiv = CLERG)
  (3) Coefficient of the Achenbach term in the generalized Ergun equation.
  (default = 0.0, units = dimensionless, equiv = CCACH)
  (4) Exponent in the Achenbach term in the generalized Ergun equation.
  (default = 0.4, units = dimensionless, equiv = CPACH)
  (5) Minimum porosity to be used in evaluating the correlation, imposed as a bound before K_{eff} is evaluated.
  (default = 0.05, units = dimensionless, equiv = PORMIN)

- 4414 - Minimum Hydrodynamic Volume Fraction: This parameter defines a fraction of the initial hydrodynamic volume in each segment of the volume/altitude table of a control volume (as specified on the CVH_VAT records) that will be considered as available to hydrodynamic materials. This volume is preserved, regardless of virtual volume changes resulting from relocation of non-hydrodynamic materials such as core debris.
  1. Minimum fraction of the initial volume in each segment of the volume/altitude table of a control volume that will always be available to hydrodynamic materials. Default = 0.01. PB SOARCA value = 0.01

For the Fukushima UA, only the minimum porosity to be used in calculating the flow resistance and heat transfer will be varied. A uniform distribution will be used for the parameters with a lower bound of 0.01 and an upper bound of 0.2. These values were chosen to span the default value of 0.05 and be consistent with the minimum debris porosity used in the Lipinski dryout model (see Section 5.2.3).

The value for flow resistance is treated as perfectly correlated with that for heat transfer. Moreover, this value is also treated as perfectly correlated with the minimum debris porosity used in the Lipinski dryout model (see Section 5.2.3).

6 MELCOR COMPUTATIONAL UNCERTAINY

6.1 Time Step Schemes for Reliable Transient Execution

Uncertainty analyses involve the execution of hundreds to thousands of MELCOR calculations (called realizations) with varying boundary conditions and physics model inputs. In order to quantify model uncertainty, discrete values are sampled from cumulative distribution functions for each uncertain parameter and input into the MELCOR model. The variation of MELCOR physics model and boundaries condition input alters the accident progression. In particular, the in-vessel accident progression may change for each realization, and this behavior challenges the MELCOR code in unique ways not typically encountered in standalone MELCOR applications. In standalone applications, MELCOR errors are usually resolved by manually restarting the simulation from an earlier restart point and changing certain input, such as maximum time step size, in order to circumvent the MELCOR error. However in highly automated uncertainty simulations, this manual method of debugging MELCOR errors is not viable for many MELCOR calculations. The MELCOR model must be stable over a range of accident progressions in order to sufficiently sample the uncertain parameters.

In general, the in-vessel accident progression is the most computationally intensive and challenging portion of a severe accident simulation in MELCOR. Previous uncertainty studies and advanced PRA applications with MELCOR, involving thousands of distinct MELCOR simulations, have resulted in MELCOR failure rates of approximately 5% to 50% [15][25][26]. MELCOR errors are highly dependent upon the model size, nodalization, and accident sequence complexity, but most of these failures are due to thermal-hydraulic and material relocation convergence errors in the core region during in-vessel degradation. A MELCOR failure is defined as the simulation encountering a fatal MELCOR error before reaching the user-desired truncation time, which was usually 48 to 96 hours in past studies. MELCOR errors can be characterized as logical failures (i.e., something occurring that the code considers impossible) or numerical convergence failures (i.e., an iterative solution scheme to a governing equation failing to converge) that are detected by the MELCOR code; these errors should not be confused with run-time errors that are faults undetected by the code, and cause the code to exit without reporting the nature of the error to the user.

The vessel and core regions usually have the finest spatial nodalization in the MELCOR model. As the active fuel uncovers, steam oxidation reactions with Zircaloy and steel generate large amounts of heat, which accelerates the geometric degradation of structures in the core and lower vessel. The chemical reactions, material relocation, and thermal-hydraulic response in the core and lower vessel are tightly coupled phenomena in a severe accident. The in-vessel accident progression involves large releases of oxidation energy along with rapidly changing core geometry, both of which strongly effect the MELCOR calculations of the in-vessel thermal-hydraulic behavior, which in turn influences the in-vessel degradation. In uncertainty simulations the in-vessel accident progression may vary considerably due to the changing of the MELCOR model inputs and boundary conditions. Given a single input model and time step scheme, MELCOR may encounter convergence issues for a subset of all the potential in-vessel accident progressions.

MELCOR uncertainty simulations are intended to exhibit different accident progressions in order to yield a range of calculated quantities (e.g. release fraction). Because uncertainty simulations are executed in an automated fashion, a generalized time step scheme must be specified in the input that is resilient enough to facilitate the convergence of a sufficient number of simulations. In standalone MELCOR calculations, the user specifies the appropriate time step scheme on the EXEC_TIME input card, and this input may need modifying for different accident sequences and accident progressions. MELCOR can automatically reduce the size of the time step due to convergence issues in any MELCOR package, and repeat cycles with reduced time step sizes. Still, it is often beneficial for the user to manually specify a reasonable maximum time step since automatic time step reductions may sometimes fail to resolve a convergence problem. The maximum time step also cannot be so small that CPU time is unreasonable. The EXEC_DTMAXCF card is used to override the maximum allowed time step size specified on the EXEC_TIME card. The EXEC_DTMAXCF card is linked to control functions that can be used to develop logic for dynamic specification of the maximum time step size.

Based on preliminary scoping analyses, a value of 0.1 s will be used as the value for the maximum time-step size in the initial UA simulations. This value was found to be sufficiently small such that convergence errors can be avoided and yet still allow the simulations to complete in a reasonable time frame Further UA studies or supplementary sensitivity calculations can identify optimum time-step schemes for reliable code execution and convergence using the control function approach linked with the EXEC_DTMAXCF input record.

6.2 Core Nodalization

In MELCOR, the core region includes a cylindrical space extending vertically downward along the inner surface of the core shroud from the core top guide to the reactor vessel lower head. It also extends radially outward from the core shroud to the hemispherical lower head in the region of the lower plenum below the base of the downcomer, preserving the curvature of the lower head from this point back to the vessel centerline.

The core and lower plenum regions are divided into concentric radial rings and axial levels. Each core cell may contain one or more core components, including fuel pellets, cladding, canister walls, supporting structures (e.g., the lower core plate and control rod guide tubes), non-supporting structures (e.g., control blades, the upper tie plate, and core top guide) and once fuel damage begins, particulate and molten debris.

The spatial nodalization of the core is shown in Figure 13. The entire core and lower plenum regions are divided into six radial rings. The radial distance between each of the five rings is not uniform. Radial ring 6 represents the region in the lower plenum outside of the core shroud and below the downcomer. Ring 6 exists only at the lowest axial levels in the core model.

The core and lower plenum are divided into 17 axially stacked levels. The height of a given level varies but generally corresponds to the vertical distance between major changes in the flow area, structural materials, or other physical features of the core (and below core) structures. Axial levels 1 through 5 represent the open space and structures within the lower plenum. Initially, this region has no fuel and no internal heat source but contains a considerable mass of steel associated with the control rod guide and in-core instrument tubes. During the core degradation process, the fuel, cladding, and other core components displace the free volume within the lower plenum as they relocate downward in the form of particulate or molten debris.

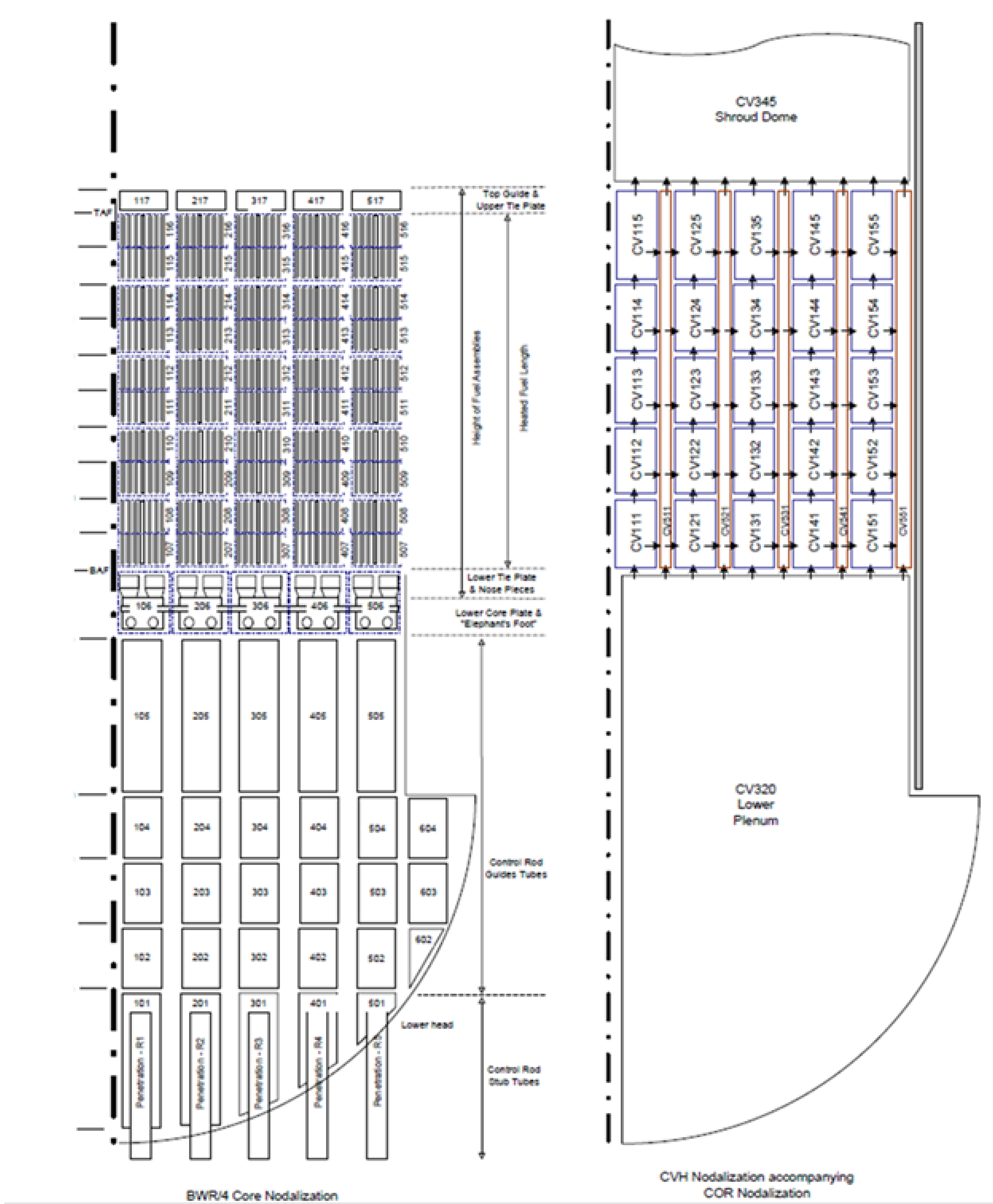

Figure 13. Spatial Nodalization of the Core and Lower Plenum.

Based on preliminary scoping calculations, it has been found that the nodalization scheme can influence the calculated core degradation progression. Therefore it is of interest to vary the nodalization, even if only in a limited fashion, to see the effect of its variation on model results. The preliminary plan in this regard is to evaluate the effect of varying number of axial CV cells in the active core region.

6.3 MELCOR Numerical Uncertainty

Preliminary scoping calculations have found that small variations in model input can result in large changes in model output. It is postulated that this is caused by

- Small convergence errors being "amplified" by discrete events that occur in the simulation. For example, steam dome pressure time histories that appear to be "nearly identical" will result in slightly different initial SRV opening times and closing times. This difference will increase with each SRV cycle. Similar amplification of small differences has been seen in the calculated core melt/degradation phenomena.
- As the calculation marches out in time, small convergence errors can result in MELCOR choosing different time step sizes (and subcycle time step sizes). This also acts as an "amplifier".

There may also be other issues contributing to this behavior.

The scope and schedule of the UA does not support an in-depth evaluation to determine the root cause(s) and any associated code and model modifications to resolve the issue. Instead, the preliminary plan is to attempt to heuristically quantify this numerical uncertainty by performing the following:

- Perform a COR parameter perturbation analysis in which a subset of the COR uncertain parameters and the COR sensitivity coefficients are sampled from uniform distributions with upper and lower bounds of +/-0.5% of their best-estimate/median/default values.
- Perform a maximum time-step size perturbation analysis in which the maximum time-step size is sampled from a uniform distribution with upper and lower bounds of +/-0.5% of the current maximum time-step size.

It is anticipated that each analysis will be run for between 50 to 100 realizations. Confidence bounds on key figures of merit (e.g., in-core H_2 production, time of lower head failure, core debris that moves from the RPV to the drywell) will be developed to quantify the numerical uncertainty.

7 PRELIMINARY UA CALCULATION PLAN

The Peach Bottom SOARCA UA provides the basic methodology template that will be followed for performing Fukushima UA calculations (see Figure 1).

- Uncertain parameter distributions will be defined.
- The distributions will be sampled for a sufficient number of realizations.
- The sampled values will be either directly input into the MELCOR 1F1 input deck or the sampled values (and/or MELCOR inputs derived from them) will be incorporated into the input deck via auxiliary files.

Where the Fukushima UA methodology will differ from the Peach Bottom SOARCA UA methodology is in the treatment of some of the boundary condition uncertainty, nodalization uncertainty, and numerical uncertainty. It is anticipated that these uncertainties will be sampled separately and evaluated in their own "loop" (see Figure 14).

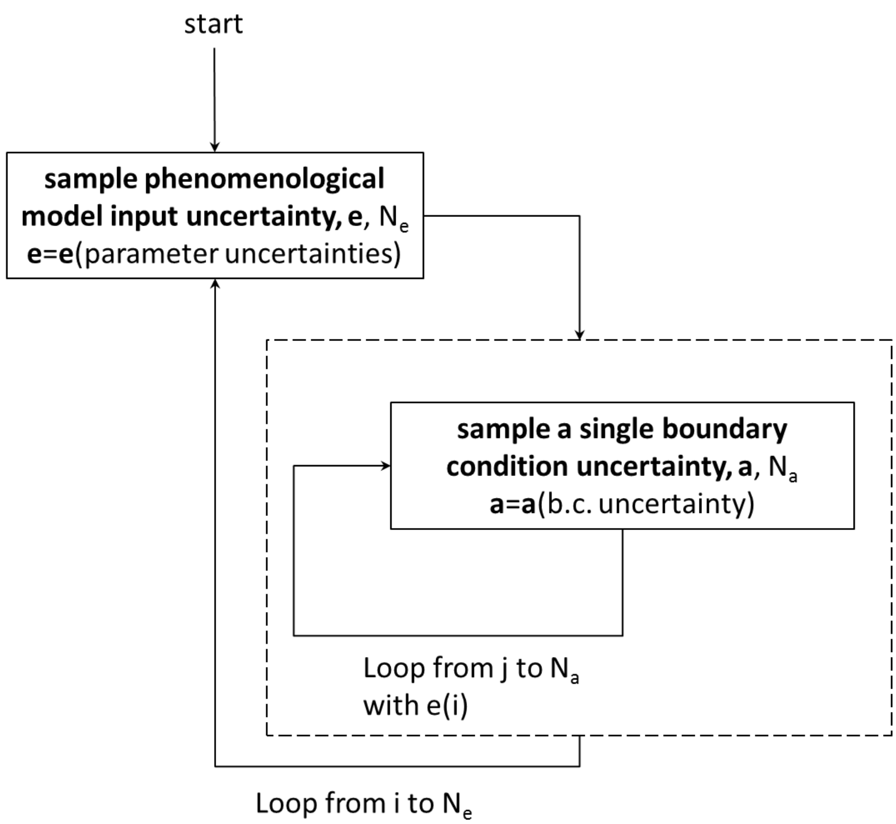

Figure 14. Outer and Inner Loop Treatment for Phenomenological and Boundary Condition Uncertainty.

Table 6 contains a preliminary list of the uncertainty analysis cases to be run for the Fukushima UA. Summaries of the preliminary phenomenological model uncertain parameters and boundary conditions uncertain parameters are provided in Table 7and Table 8.

.

Table 6. Preliminary List of Uncertainty Analysis Cases.

analysis	notes
perturbation analyses	
parameter perturbation	100 realization
maximum time-step size perturbation	100 realizations
statistical convergence analyses	
statistical convergence	three 200-realization replicate sets
phenomenological model input uncertainty	
phenomenological model input uncertainty	anticipate that this analysis will be on the order of 100 to 200 realization, statistical convergence analysis will justify the number of realizations used.
boundary condition nodalization, and numerical uncertainty analyses	
phenomenological model input uncertainty + RCS failure modes uncertainty	MLS failure, SRV failure and graphfoil seal failure using the distribution for RCS failure time
phenomenological model input uncertainty + DTMAX variation	log-uniform sampling between 0.01 and 0.1 s
physics parameter uncertainty + COR CV nodalization	anticipate evaluating cases with 5, 3 and 1 axial CVs in the each ring in the active core region

Table 7. Preliminary List of Core Phenomenological Model Uncertain Parameters.

parameter	distribution
molten zircaloy melt break-through temperature	triangle distribution LB = 2100 K mode = 2400 K UB = 2540 K
molten clad drainage rate	log-triangle distribution LB = 0.1 kg/m-s mode = 0.2 kg/m-s UB = 1.0 kg/m-s
time constants for radial (solid) debris relocation	log-triangle distribution LB = 180 s mode = 360 s UB = 720 s
time constants for radial (liquid) debris relocation	log-triangle distribution LB = 30 s mode = 60 s UB = 120 s
SC1030(2), dT/dz model, time constant for averaging flows	uniform distribution LB = 0.09 s UB = 0.11 s
SC1030(4), dT/dz model, characteristic time for coupling dT/dz temperatures to average CVH volume temperature when dT/dz model is active	uniform distribution LB = 8 s UB = 12 s
SC1030(5), dT/dz model, maximum relative weight of old flow in smoothing algorithm involving time constant for averaging flows	uniform distribution LB = 0.5 s UB = 0.7 s
fraction of strain at which lower head failure occurs	uniform distribution LB = 0.16 UB = 0.20
fraction of unoxidized cladding thickness at which thermal-mechanical weakening of oxidized cladding begins	uniform distribution LB = 0.05 UB = 0.15
fuel rod collapse time-to-failure as a function of temperature	varies uniformly between +/-50% of the SOARCA characterization (see Figure 11)
scaling factor for candling heat transfer coefficients	uniform distribution LB = 0.9 UB = 1.1
minimum debris porosity (Lipinski dryout model)	uniform distribution LB = 0.1 UB = 0.2
debris quenching heat transfer coefficient to pool	uniform distribution LB = 100.0 W/m^2 K UB = 2000.0 W/m^2 K
debris quenching debris falling velocity	log-uniform distribution LB = 0.01 UB = 1.0
blockage model minimum porosity	uniform distribution LB = 0.025 UB = 0.100

Table 8. Preliminary List of Boundary Condition Uncertain Parameters.

analysis	notes
RCS pressure boundary failure time	uniform distribution LB = 5.5 hr UB = 6.5 K
model of RCS pressure boundary failure	equally weighted between: main steam line failure safety relief valve failure safety relief valve grapfoil seal failure
water injection rate scaling parameter(1)	uniform distribution LB = 0.05 UB = 0.25
upper drywell head flange leakage: non-zero leakage threshold pressure and dA/dp relationship(1)	uniform distributions LB = -10% of calibrated base case UB = +10% of calibrated base case
decay heat time history(1)	uniform sampling of from set of decay heat time-histories

(1) While boundary conditions, these parameters fit in better with the phenomenological model input uncertain parameters, and will be included in their “loop”.

8 SUMMARY

A preliminary set of uncertain parameters have been selected for 1F1 uncertainty analysis. A preliminary uncertainty analysis methodology has also been identified. Documentation (i.e., this SAND report) of the preliminary uncertain parameters and methodology has been created and will be provided to stakeholders (e.g., DOE, NRC, EPRI, BSAF participants, etc.) for their review upon it promulgation.

REFERENCES

1. R.O. Gauntt, et al., NUREG/CR-6119, "MELCOR Computer Code Manuals, Vol. 2: Reference Manuals, Version 1.8.6 (Vol. 2, Rev. 3)," Sandia National Laboratories, Albuquerque, NM, 2005.
2. R.O. Gauntt, D.A. Kalinich, et al., “Fukushima Daiichi Accident Study,” SAND2012-6173, Sandia National Laboratories: Albuquerque, NM (2012).
3. R.O. Gauntt, D.A. Kalinich, et al., “MELCOR Simulations of the Severe Accident at the Fukushima 1F1 Reactor,” Proceedings of 2012 ANS Winter Meeting & Nuclear Technology Expo, San Diego, CA, November 11-15 (2012).
4. J. Phillips, J.N. Cardoni, et al., “MELCOR Simulations of the Severe Accident at the Fukushima 1F2 Reactor,” Proceedings of 2012 ANS Winter Meeting & Nuclear Technology Expo, San Diego, CA, November 11-15 (2012).
5. J.N. Cardoni, R.O. Gauntt, et al., “MELCOR Simulations of the Severe Accident at the Fukushima 1F3 Reactor,” Proceedings of 2012 ANS Winter Meeting & Nuclear Technology Expo, San Diego, CA, November 11-15 (2012).
6. D. Luxat and J. Gabor “Fukushima Technical Evaluation: Phase 1– MAAP5 Analysis,” EPRI Final Report 1025750, Palo Alto, CA, April (2012).
7. M. Braun and G. Urzua, “MELCOR 1.8.6 Analysis of the Core Degradation in the Fukushima Daiichi Power Plant,” Severe Accident Research Program and MELCOR Code Assessment Program (MCAP2011), Bethesda, MD, September 20-23 (2011).
8. TEPCO, “MAAP Code-based Analysis of the Development of the Events at the Fukushima Daiichi Nuclear Power Station,” http://www.tepco.co.jp/en/nu/fukushima-np/images/handouts_120312_04-e.pdf (2012).
9. H. Hoshi, et al., “Severe Accident Analyses of Fukushima-Daiichi Units 1 to 3,” Proceedings of 2012 Fukushima Ministerial Conference on Nuclear Safety, Fukushima Prefecture, Japan, December 15-17 (2012).
10. K. Robb, et al., “Fukushima Daiichi Unit 3 MELCOR Investigation,” Proceedings of 2012 ANS Winter Meeting & Nuclear Technology Expo, San Diego, CA, November 11-15 (2012).
11. M. Pellegrini, et al., “Analysis of Accident Progression of Fukushima Dai-ichi with SAMPSON Code—(3) Unit 3,” Proceedings of 2012 ANS Winter Meeting & Nuclear Technology Expo, San Diego, CA, November 11-15 (2012).
12. D.I. Chanin and M.L. Young, NUREG/CR-6613, "Code Manual for MACCS2: Volume 1, User's Guide," U.S. Nuclear Regulatory Commission, Washington, DC (1997).
13. U.S. NRC, “State-of-the-Art Reactor Consequence Analysis (SOARCA) Report,” NUREG/CR-7110, U.S. Nuclear Regulatory Commission: Washington D.C. 2012.
14. J.C. Helton, et al., "Survey of Sampling-based Methods for Uncertainty and Sensitivity Analysis," Reliability Engineering & System Safety, 91(10-11): p. 1175-1209, 2006.

15. U.S. NRC, “State-of-the-Art Reactor Consequence Analyses Project, Uncertainty Analysis of the Unmitigated Long-Term Station Blackout of the Peach Bottom Atomic Power Station,” NUREG/CR-7155, DRAFT REPORT (SAND2012-10702P), 2012.

16. R.O. Gauntt, “Synthesis of VERCOS and Phebus data in Severe Accident Codes and Applications,” SAND2010-1633, Sandia National Laboratories, April 2010.

17. Hanniet-Girault, N. and G. Repetto, "PHEBUS FPT0 Final Report," Cadarache, France, 1998.

18. Jacquemain, D., et al., "PHEBUS FPT1 Final Report," Cadarache, France, 2000.

19. Gregoire, A.C., P. Chapelot, and G. Gregoire, "PHEBUS FPT4 Final Report," Cadarache, France, 2004.

20. Gregoire, A.C., "PHEBUS FPT2 Final Report," Cadarache, France, 2008.

21. Pavot, F., et. al., "PHEBUS FPT3 Final Report," Cadarache, France, 2010.

22. R.O. Gauntt, R.D. Gasser, “Results of the DF-4 BWR Control Blade-Channel Box Test,” SAND90-2716C, Sandia National Laboratories: Albuquerque, NM (1990).

23. R.O. Gauntt, et al., “Final Results of the XR2-1 BWR Metallic Melt Relocation Experiment,” SAND97-1039 (NUREG/CR-6527), Sandia National Laboratories: Albuquerque, NM (1990).

24. R.O. Gauntt, et al., NUREG/CR-6119, "MELCOR Computer Code Manuals, Vol. 1: Primer and User's Guide, Version 1.8.6 (Vol. 1, Rev. 3)," Sandia National Laboratories, Albuquerque, NM, 2005.

25. J. LaChance, J.N. Cardoni, et al., “Discrete Dynamic Probabilistic Risk Assessment Model Development and Application,” SAND2012-9346, Sandia National Laboratories, Albuquerque, NM, October 2012.

26. M.R. Denman, J.N. Cardoni, et al., “Discrete Dynamic Event Tree Capability Study for Advanced Small Modular Reactors,” SAND2013-2514, Sandia National Laboratories, Albuquerque, NM, March 2013.

27. TEPCO strip chart data available from the TEPCO website: http://www.tepco.co.jp/nu/fukushima-np/index10-j.html, accessed April 4, 2013.

28. TEPCO, “Preliminary survey in Torus Room of Units 2 and 3,” http://www.tepco.co.jp/en/nu/fukushima-np/images/handouts_120314_01-e.pdf, accessed April 3, 2013.

29. TEPCO, “Units 1-2 Torus Room Investigation at Fukushima Daiichi Nuclear Power Station,” http://www.tepco.co.jp/en/nu/fukushima-np/handouts/2013/images/handouts_130125_02-e.pdf, accessed April 4, 2013.

30. TEPCO, “Fukushima Daiichi Nuclear Power Station Unit 3 Reactor Building Basement Torus Room Investigation,” http://www.tepco.co.jp/en/nu/fukushima-np/images/handouts_120712_03-e.pdf, accessed April 4, 2013.

31. T. Downar, “Nuclear Fuel Cycle: Nuclear Source Characterization,” Purdue University, March 2005.

32. P. Finck, D. Keyes, and R. Stevens, "Workshop on Simulation and Modeling for Advanced Nuclear Energy Systems," Washington, D.C., August 15-17 (2006). http://science.energy.gov/~/media/ascr/pdf/program-documents/docs/Gnep_06_final.pdf

33. R.O. Gauntt, N. Bixler, and K.C. Wagner, "An Uncertainty Analysis of the Hydrogen Source Term for a Station Blackout Accident in Sequoyah Using MELCOR 1.8.5 (Draft For Review)," Sandia National Laboratories, Albuquerque, NM, 2003.

34. TEPCO Press Release, "The Estimated Amount of Radioactive Materials Released into the Air and the Ocean Caused by Fukushima Daiichi Nuclear Power Station Accident Due to the Tohoku-Chihou-Taiheiyou-Oki Earthquake (As of May 2012)," http://www.tepco.co.jp/en/press/corp-com/release/2012/1204659_1870.html (2012).

35. TEPCO, "Method of Estimation of the Released Amount of Radioactive Materials into the Atmosphere," http://www.tepco.co.jp/en/press/corp-com/release/betu12_e/images/120524e0203.pdf (2012).

36. Scale: A Comprehensive Modeling and Simulation Suite for Nuclear Safety Analysis and Design. ORNL/TM-2005/39, Version 6.1, June 2011. Available from Radiation Safety Information Computational Center at Oak Ridge National Laboratory as CCC-785.

37. L.L. Humphries, et al., "OECD Lower Head Failure Project: Final Report," NEA/CSNI/R(2002)27, (2002).

38. S. Ergun, "Fluid Flow Through Packed Columns," *Chemical Engineering Progress,* **48**(2), 89-94, 1952.

39. R. Lipinski, "A Coolability Model for Post-Accident Nuclear Reactor Debris," Nuclear Technology, **65**, 53-66, 1984.

APPENDIX A COR MODELS AND SENSITIVITY COEFFICIENTS

This appendix contains a nearly-complete listing of the MELCOR COR models and associate sensitivity coefficients.

Sub-models in COR Heat Transfer and Oxidation Modeling

Radiation

- Emissivity
- View Factors

Conduction

- Axial Temperature Profile
- Axial Conduction in a component within a COR cell
- Quench Front Velocity Model
- Axial Conduction between components in different COR Cells
- Radial Conduction
- Other Intra-cell Conduction
- Fuel Cladding Gap Heat Transfer
- Consideration of Heat Capacity of components
- Effective Heat Capacity of Cladding
- Conduction to Boundary Heat Structures

Convection

- Laminar Forced Convection
- Turbulent Forced Convection
- Laminar and Turbulent Free Convection
- Convection from Particulate Debris
- Boiling

- Heat Transfer from horizontal surfaces of plates
- Debris Quenching and Dryout

Molten Pool Heat Transfer

- Contiguous Physical Molten Pools
- Convection Heat Transfer
- Heat Transfer to underlying substrate from molten pool (heat-up of substrate, and either ablation, or freezing)

Oxidation

- Zircaloy and Steel
- Simple/Advanced Boron Carbide Reaction Model
- New B_4C Control Rod Oxidation Model
- Steam/Oxygen Allocation

Control Volume Temperature Distribution (dT/dz) Model

Material Interactions (Eutectics)

- Mixture Formation
- Mixture Properties
- Chemical Dissolution of Solids

<u>Sub-models in Core/In-Vessel Material Relocation Modeling</u>

Candling

- Steady Flow
- Flow Blockages
- Holdup of Oxide Shells
- Solid Material Transport
- Radial Relocation of Molten Materials

- Surface Area Effect of Conglomerate Debris

Particulate Debris
- Formation of Particulate Debris – transition from fuel assembly geometry
    - Multiple criteria for loss of rod geometry
- Debris addition from Heat Structure Melting
- Exclusion of Particulate Debris
- Radial Relocation of Particulate Debris
- Gravitation Settling

Molten Pool
- Slumping and Displacement
- Contiguous Molten Pools
- Partitioning of Radionuclides

Displacement of Fluids in CVH

<u>Sub-models in COR Support Structure and Non-supporting Structure Models</u>

Model for Intact PWR Core Shroud (baffle) and Core Formers

Models for Stainless Steel
- PLATEG Model – grid/beam-supported plate
- PLATE Model – basic edge-supported plate
- PLATEB Model – BWR-specific core plate: does not support the core (the weight of the core is transferred to the guide tubes) but can hold up particulate debris
- COLUMN Model

Stainless steel Failure Models
- Failure by Yielding
- Failure by Buckling

- Failure by Creep

Lower Head Model

- Heat Transfer
- Failure
- Debris Ejection

COR MODEL INPUTS, SENSTIVITY COEFFICENTS, AND OUTPUTS

Core Material Relocation Models

INPUTS
Zr mass & solidus/ liquidus (from COR)
ZrO_2 mass & solidus/ liquidus (from COR)
UO_2 mass & solidus/ liquidus (from COR)
SS mass & solidus/ liquidus (from COR)
SS-oxide mass & solidus/ liquidus (from COR)
B_4C mass & solidus/ liquidus (from COR)
Inconel mass & solidus/ liquidus (from COR)
Temperature of surface(s) (from COR)
CV temperature & volume (from CV)
Fe, Cr, Ni, C steel mass fractions (from MP)

SENSITIVITY COEFFICIENTS
1020 – Radial Relocation Model Parameters

- Solidus (default = 360 sec)
- Liquidus (default = 60 sec)
- Lower head curvature bias for solidus (default = not used)
- Lower head curvature bias for liquidus (default = not used)
- Fraction of cell CVH volume available for radial relocation (default = 1)

1021 – Channel-Bypass Relocation Time Constant

OUTPUTS
Zr mass loss (taken from component (COR))
ZrO_2 mass loss (taken from component (COR))
UO_2 mass loss (taken from component (COR))
SS mass loss (taken from component (COR))
SS-oxide mass loss (taken from component (COR))
B_4C mass loss (taken from component (COR))
Inconel mass loss (taken from component (COR))

Zircaloy (Zr), Steel (SS), and Boron Carbide (B_4C) Oxidation

INPUTS
Zr mass (from COR)
SS mass (from COR)
B_4C mass (from COR)
H_2O mass (from steam/oxygen allocation model)

O_2 mass (from steam/oxygen allocation model)
Temperature of surface(s) (from COR)
CV temperature (from CV)
CV flow rates (from CV)
Fe, Cr, Ni, C steel mass fractions (from MP)

SENSITIVITY COEFFICIENTS
1001 – Zircaloy Oxidation Rate Constant Coefficients
1002 – Steel Oxidation Rate Constant Coefficients
1003 – Gaseous Diffusion Oxidation Coefficients (Zr and SS)
1004 – Oxidation Cutoff Temperatures (Zr and SS)
1005 – B_4C Reaction Model Parameters

- Maximum B_4C fraction that may be consumed by the reaction model (default = 0.02)
- Intact steel failure fraction. The B_4C reaction cannot begin until the ratio of the intact steel mass to its initial value falls below this fraction (default = 0.9)
- Reaction threshold temperature. The B_4C temperature must exceed this value or the reaction cannot proceed (default = 1500 K)

1006 – B_4C Reaction Rate Parameters
1007 – Ring Minimum Flow Area Fractions

- Minimum flow area fraction on channel-side (default = 0)
- Minimum flow area fraction on bypass-side (default = 0)

OUTPUTS
Reduction in Zr mass (taken from component (COR))
Reduction in SS mass (taken from component (COR))
Reduction in B_4C mass (taken from component (COR))
Reduction in steam mass (taken from steam/oxygen allocation model)
Reduction in O_2 mass (taken from steam/oxygen allocation model)
ZrO_2 mass generated (added to component (COR))
SSOX mass generated (added to component (COR))
B_2O_3 mass generated (added to RN package as an aerosol)
H_2 mass generated (added to CV (CVH))
CO mass generated (added to CV (CVH))
Zr oxidation energy generated (added to component (COR))
SS oxidation energy generated (added to component (COR))
B_4C oxidation energy generated (added to CV (CVH))
Fraction of oxidized inventory (added to component (COR))

<u>Material Interactions (Eutectics)</u>

INPUTS
Zr mass & Temperature (from COR)
ZrO_2 mass & Temperature (from COR)
UO_2 mass & Temperature (from COR)
SS mass & Temperature (from COR)
SS-oxide mass & Temperature (from COR)
B_4C mass & Temperature (from COR)
Inconel mass & Temperature (from COR)
Temperature of surface(s) (from COR)
CV temperature (from CV)
Fe, Cr, Ni, C steel mass fractions (from MP)

SENSITIVITY COEFFICIENTS
1010 – Material Dissolution Rate Coefficients - These coefficients are used to limit the rate of dissolution of materials by parabolic kinetics.
1011 – Eutectic Reaction Temperatures

- Zirc-Inconel (default = 1400K)
- Zirc-steel (default = 1400K)
- Steel-B_4C (default = 1520K)

OUTPUTS
Zr mass loss (taken from component (COR))
ZrO_2 mass loss (taken from component (COR))
UO_2 mass loss (taken from component (COR))
SS mass loss (taken from component (COR))
SS-oxide mass loss (taken from component (COR))
B_4C mass loss (taken from component (COR))
Inconel mass loss (taken from component (COR))

Breakaway Air-Oxidation Model

INPUTS
Zr mass & Temperature (from COR)
H_2O mass (from steam/oxygen allocation model)
O_2 mass (from steam/oxygen allocation model)
Temperature of surface(s) (from COR)
CV temperature (from CV)
CV flow rates (from CV)

SENSITIVITY COEFFICIENTS
1016 – Zircaloy Post-Breakaway Oxidation Rate Constant Coefficients
1017 – Lifetime Parameters for Breakaway Model
1018 – Maximum Lifetime for Breakaway Model

OUTPUTS
Zr mass loss (taken from component (COR))
ZrO_2 mass created (input to component (COR))

Control Volume Temperature Distribution

INPUTS
H_2O temperature (from CV)
O_2 temperature (from CV)
H_2 temperature (from CV)
N_2 temperature (from CV)
CH_2 temperature (from CV)
CO_2 temperature (from CV)
CO temperature (from CV)
Temperature & area of surface(s) (from COR)
CV gas temperature & gas flow rates (from CV)
Fission product decay heat (from COR)
B_4C reaction energy (from COR)

SENSITIVITY COEFFICIENT
1030 – dT/dz Model Parameters

6. Option switch (default = older than MELCOR 1.8.3 version)

7. Time constant for averaging flows (default = 0.1 sec)

8. Time constant for relaxing dT/dz temperatures towards CVH volume temperature when dT/dz model is disables (default = 1.0 sec)

9. Characteristic time for coupling dT/dz temperatures to average CVH volume temperature when dT/dz model is active (default = 10 sec)

10. Maximum relative weight of old flow in smoothing algorithm involving time constant for averaging flows (default = 0.6)

OUTPUTS
H_2O temperature (outlet of CV)
O_2 temperature (outlet of CV)
H_2 temperature (outlet of CV)
N_2 temperature (outlet of CV)
CH_2 temperature (outlet of CV)

CO_2 temperature (outlet of CV)
CO temperature (outlet of CV)
CV gas temperature & gas flow rates (outlet of CV)

Emissivity

INPUTS
Zr temperature (from COR)
ZrO_2 temperature (from COR)
UO_2 temperature (from COR)
SS temperature (from COR)
SS-oxide temperature (from COR)
B_4C temperature (from COR)
Inconel temperature (from COR)
Graphite temperature (from COR – if applicable)

SENSITIVITY COEFFICIENT
1101 – Fuel Emissivity & Cladding Gap Emissivity
Single Point Estimate (default = 0.8 – Fuel surface & 0.325 – Cladding inner surface)
1102 – Steel Emissivity (default values duplicate the correlations used in MELCOR 1.8.5 for 650 ^oF)

- Range of 0.0001 to 0.9999 with reference value = 0.25617

- *Check default temperature coefficient* (0.000193/^{o}F to 0.0003474/K)

1103 – Particulate Emissivity (default values duplicate the correlations used in MELCOR 1.8.5 for a constant value of 0.9999)

- Range of 0.0001 to 0.9999 with reference value of 0.9999 and temperature coefficient of 0.0 (i.e., constant value)

1104 – Oxidized Zircaloy Emissivity (default values duplicate the correlations used in MELCOR 1.8.5 for oxide thickness of less than 1 mm)

- Range of 0.325 to 0.999

- The extrapolation of the original correlation to a very large oxide thickness could return a negative value; the correlation is cut off (by default) at an oxide thickness of 1 mm.

1105 – Graphite Emissivity

OUTPUTS
Zr temperature (from COR)
ZrO_2 temperature (from COR)
UO_2 temperature (from COR)
SS temperature (from COR)
SS-oxide temperature (from COR)
B_4C temperature (from COR)

Inconel temperature (from COR)
Graphite temperature (from COR – if applicable)

Material Holdup/Failure Parameters

INPUTS
ZrO_2 thickness (from COR)
ZrO_2 temperature (from COR)
SS-oxide thickness (from COR)
SS-oxide temperature (from COR)

SENSITIVITY COEFFICIENT
1131 – Molten Material Holdup Parameters

- Define conditions in which molten material will be held up by an oxide shell

1132 – Core Component Failure Parameters

- Temperature oxidized fuel rods can stand w/o unoxidized Zr in cladding (2500K)
- Temperature fuel rods will fail regardless of clad composition (3100K)

OUTPUTS
Zr mass loss (taken from component (COR))
ZrO_2 mass loss (taken from component (COR))
UO_2 mass loss (taken from component (COR))
SS mass loss (taken from component (COR))
SS-oxide mass loss (taken from component (COR))
B_4C mass loss (taken from component (COR))
Inconel mass loss (taken from component (COR))

Core Melt Breakthrough Candling Parameters

INPUTS
Zr mass that enters the COR cell on the surfaces
ZrO_2 mass that enters the COR cell on the surfaces
UO_2 mass that enters the COR cell on the surfaces
SS mass that enters the COR cell on the surfaces
SS-oxide mass that enters the COR cell on the surfaces
B_4C mass that enters the COR cell on the surfaces
Inconel mass that enters the COR cell on the surfaces

SENSITIVITY COEFFICIENT
1141 – Core Melt Breakthrough Candling Parameters

- Timestep size used in candling model for molten material releases immediately after breakthrough of an oxide shell or crust (1 sec)

- Maximum melt flow rate per unit width after breakthrough (1 kg/s-m)

Default values allow the model to be active ***ONLY*** for large molten pools breaching a crust.

OUTPUTS
Zr mass loss (taken from component (COR))
ZrO_2 mass loss (taken from component (COR))
UO_2 mass loss (taken from component (COR))
SS mass loss (taken from component (COR))
SS-oxide mass loss (taken from component (COR))
B_4C mass loss (taken from component (COR))
Inconel mass loss (taken from component (COR))

Surface Area Parameters

INPUTS
Intact fuel
Intact cladding
Intact canister portion not adjacent to a control blade (BWR)
Intact canister portion adjacent to a control blade (BWR)
'Other Structure'
Particulate debris portion in the channel (BWR)
Supporting structure component
Non-supporting structure component
Particulate debris component in the bypass (BWR)

SENSITIVITY COEFFICIENT
1151 – Conglomerate Debris Surface Area Coefficients

- A candling parameter – calculates the surface area of conglomerate debris and the portion of the intact component surface area that remains unblocked by the conglomerate debris (only used in the component oxidation models)

- Default values are based on typical BWR rod geometries with pitch 16 mm and rod radius 6.26 mm.

1152 – Surface to Volume Ratio for Fluid

- Limits the surface area for heat transfer from COR to CVH when core is blocked and the fluid volume is very small (1000 m^{-1} is the default)

OUTPUTS
Reduction in Zr mass (taken from component (COR))
Reduction in SS mass (taken from component (COR))
Reduction in B_4C mass (taken from component (COR))
Reduction in steam mass (taken from steam/oxygen allocation model)
Reduction in O_2 mass (taken from steam/oxygen allocation model)
ZrO_2 mass generated (added to component (COR))
SSOX mass generated (added to component (COR))
B_2O_3 mass generated (added to RN package as an aerosol)
H_2 mass generated (added to CV (CVH))
CO mass generated (added to CV (CVH))
Zr oxidation energy generated (added to component (COR))
SS oxidation energy generated (added to component (COR))
B_4C oxidation energy generated (added to CV (CVH))
Fraction of oxidized inventory (added to component (COR))

Heat Transfer Coefficient Smoothing

INPUTS
Temperature of surface(s) (from COR)
CV temperature (from CV)

SENSITIVITY COEFFICIENT
1200 – Smoothing of Heat Transfer Coefficients

- Correlates heat transfer between surfaces of COR components and surrounding atmosphere and/or pool are averages with the values from previous timesteps:

$$h_{new} = f_{old}h_{old} + (1 - f_{old})h_{calc}$$

- Defaults
  - 0.5 weight for old heat transfer to atmosphere
  - 0.9 weight for old heat transfer to pool from quenched surfaces
  - 0.9 weight for old heat transfer to pool from unquenched surfaces (not used in current implementation where this coefficient is a constant)

OUTPUTS
Temperature of surface(s) (from COR)
CV temperature (from CV)

Laminar, Turbulent, and Forced Flow

INPUTS
CV flow rates (from CV)

SENSITIVITY COEFFICIENT
1212 – Laminar Nusselt Numbers

- Coefficients which give the constant Nusselt number for various types of laminar forced convective flow

1213 – Laminar Developing Flow

- Coefficients used to calculate a developing flow factor for laminar flow

1214 – Turbulent Forced Convective Flow in Tubes

- Coefficients used to calculate the Nusselt number for forced convective flow in tubes

1221 – Laminar Free Convection between Parallel Vertical Surfaces

- Coefficients use to calculate the Nusselt number for Laminar free convection between parallel vertical surfaces

1222 – Turbulent Free Convection between Parallel Vertical Surfaces

- Coefficients used to calculate the Nusselt number for turbulent free convection between parallel vertical surfaces

1231 – Forced Convective Flow over a Spherical Particle

- Coefficients used to calculate the Nusselt number for forced convective flow over a single spherical particle

1232 – Free Convective Flow over a Spherical Particle

- Coefficients used to calculate the Nusselt number for free convective flow over a single spherical particle

OUTPUTS
CV flow rates (from CV)

Nucleate Boiling & Dryout

INPUTS
Temperature of surface(s) (from COR)
CV temperature (from CV)
CV pressure (from CV)

SENSITIVITY COEFFICIENT
1241 – Simplified Nucleate Boiling Curve

- Coefficients used to calculate a simplified nuclear boiling curve for pool boiling
- Must change a constant, C1241(5), to nonzero for this sensitivity coefficient to apply

1242 – Simplified Transition Film Boiling Curve

- Coefficients used to calculate a simplified transition boiling curve for pool boiling
- Must change a constant, C1241(5), to nonzero for this sensitivity coefficient to apply

OUTPUTS
Temperature of surface(s) (from COR)
CV temperature (from CV)
CV pressure (from CV)

Lower Head Heat Transfer & Dryout

INPUTS
Lower head temperature of surface(s) (from CV)
CV temperatures (from CV)

CV liquid and gas density

SENSITIVITY COEFFICIENT
1244 – Debris Dryout Heat Flux Correlation

- Coefficients use to calculate the Dryout heat flux for particle debris beds
    - *Section 2.3.8 of Reference Manual*

1245 – Downward-Facing Lower Head Heat Transfer Correlations

- Coefficients used to calculate downward heat transfer from the lower heat to water in the reactor cavity

1246 – Heat Transfer Coefficient, Lower Head to Atmosphere

- Coefficient defines the heat transfer coefficient between the lower head and the atmosphere when the head is not completely covered by pool

1250 – Conduction Enhancement for Molten Components

- Coefficients used to enhance heat transfer at high temperatures, where core debris is molten, to capture the qualitative effects of convection in molten pools

OUTPUTS
Lower heat temperature of surface(s) (from CV)
CV temperatures (from CV)

<u>Quench Model</u>

INPUTS
Temperature of surface(s) (from CV)
Saturation temperature (from CV)
CV temperatures (from CV)
Surface thicknesses (from CV)

SENSITIVITY COEFFICIENT
1260 – Quench Model Parameters

- Coefficients used with re-flooding model in the correlation for quench front velocity, and heat transfer from unquenched submerged surfaces

OUTPUTS
Temperature of surface(s) (from CV)
CV temperatures (from CV)

<u>COR Package Flow Regime Map</u>

INPUTS
CV temperature & volume (from CV)
H_2O mass water/steam (from steam/oxygen allocation model)

SENSITIVITY COEFFICIENT
1270 – Flow Regime Map Parameters

- Coefficients used to allow COR package to infer a two-phase mixture level different from that calculated by the CVH package

OUTPUTS
CV temperature (from CV)
H_2O mass water/steam (from steam/oxygen allocation model)

Molten Pool Modeling

INPUTS
Temperature of surface(s) (from CV)
CV temperatures (from CV)
CV flow rates (from CV)
Timestep (from EXEC)
Lower head radius (from CV)

SENSITIVITY COEFFICIENT
1280 – Nusselt-Rayleigh Correlation for Molten Pool

- Coefficients used to define the Nusselt-Rayleigh correlation for the convection in each molten pool

1281 – Molten Pool Convection Inertial Time Constant

- Coefficients used to define the inertial time constant for the convection of molten pools

1290 – Molten Pool Convection Model Direction Parameters

- Coefficients used to define the curve fit parameters for the molten pool convection model direction dependence used for the Nusselt number directional dependence as a function of polar angle

OUTPUTS
Temperature of surface(s) (from CV)
CV temperatures (from CV)
CV flow rates (from CV)

General & Candling Numerical Control Parameters

INPUTS
Timestep (from EXEC)
COR cell energy (from COR)
CVH energy (from CVH)
Zr mass & solidus/ liquidus (from COR)
ZrO_2 mass & solidus/ liquidus (from COR)
UO_2 mass & solidus/ liquidus (from COR)
SS mass & solidus/ liquidus (from COR)
SS-oxide mass & solidus/ liquidus (from COR)
B_4C mass & solidus/ liquidus (from COR)
Inconel mass & solidus/ liquidus (from COR)

SENSITIVITY COEFFICIENT
1401 – Timestep Control Parameters

- Coefficients used to control the system timestep to prevent instabilities in the interface between the COR and CVH packages

1402 – Candling Control Parameter

- Controls the fraction of material in a component that must be molten before it is considered available to candle

OUTPUTS
Zr mass loss (taken from component (COR))
ZrO_2 mass loss (taken from component (COR))
UO_2 mass loss (taken from component (COR))
SS mass loss (taken from component (COR))
SS-oxide mass loss (taken from component (COR))
B_4C mass loss (taken from component (COR))
Inconel mass loss (taken from component (COR))

Geometric Parameters

INPUTS
COR geometry
COR material masses
Porosity (COR or MP)

SENSITIVITY COEFFICIENT
1501 – Canister Mass/Surface Area Splits

- Specify the fraction of the input values for canister mass and surface area that are assigned to the two canister components
    - Adjacent to the control blade; the other not (default is 50/50)

1502 – Minimum Component Masses

- Specify the minimum component mass below which the masses and energies will be discarded (default = 1.0E-06 kg)
- Specify the minimum component mass below which the component will not be subject to the maximum temperature change criterion (default = 10 kg)

1503 – Core Blockage Parameters

- Replaced by 1505 parameter array – ***No longer used***

1504 – Core Cell Volume Consistency Tolerances

- Specify the tolerances on internal consistency in the representation of volumes within the COR package database

1505 – Core Blockage Parameters

- Specify the geometric parameters affecting the core flow resistance and heat transfer under conditions of flow blockage (default minimum porosity = 0.05, ***Reference manual says*** $\boldsymbol{10^{-3}}$ – Section 3.1.2)

OUTPUTS
Zr mass (from COR)
ZrO_2 mass (from COR)
UO_2 mass (from COR)
SS mass (from COR)
SS-oxide mass (from COR)
B_4C mass (from COR)
Inconel mass (from COR)

<u>Lower Head Mechanical Model Parameters</u>

INPUTS
CV pressures (from CV)
CV temperatures (from CV)
Lower head temperature of surface(s) (from CV)
Lower head material properties (from MP)
Support structure material properties (from MP)

SENSITIVITY COEFFICIENT
1600 – Model Parameters
- Specify desired level of modeling detail
    - 0-D or 1-D stress and strain distribution
    - Linear expansivity of lower head load bearing material (only applies to 1-D model)
    - Differential pressure lower limit

1601 – Larson-Miller Creep Rupture Parameters for Vessel Steel
- Default values are typical for reactor vessel carbon steel

1602 – Vessel Steel Elastic Modulus Parameters
1603 – Vessel Steel Yield Stress Parameters
1604 – Larson-Miller Creep Rupture Parameters for Support Structure
- Default values are typical for stainless steel

1605 – Internal Steel Elastic Modulus Parameters
1606 – Internal Steel Yield Stress Parameters

OUTPUTS
Lower head temperature of surface(s) (from CV)
Timing of when the lower head fails (MELCOR message)

Distribution

Internal Distribution

1	MS0748	Jeff Cardoni	06232 *(electronic copy)*
1	MS0748	Randall Gauntt	06232 *(electronic copy)*
1	MS0748	Donald Kalinich	06232 *(electronic copy)*
1	MS0748	Jesse Phillips	06232 *(electronic copy)*
1	MS0899	Technical Library	9536 *(electronic copy)*

Sandia National Laboratories